

# Dynamical Tides in Rotating Binary Stars

Dong Lai

Theoretical Astrophysics, 130-33, California Institute of Technology  
Pasadena, CA 91125  
E-mail: dong@tapir.caltech.edu

## ABSTRACT

We study the effect of rotation on the excitation of internal oscillation modes of a star by the external gravitational potential of its companion. Unlike the nonrotating case, there are difficulties with the usual mode decomposition for rotating stars because of the asymmetry between modes propagating in the direction of rotation and those propagating opposite to it. For an eccentric binary system, we derive general expressions for the energy transfer  $\Delta E_s$  and the corresponding angular momentum transfer  $\Delta J_s$  in a periastron passage when there is no initial oscillation present in the star. Except when a nearly precise orbital resonance occurs (i.e., the mode frequency equals multiple of the orbital frequency),  $\Delta E_s$  is very close to the steady-state mode energy in the tide in the presence of dissipation. It is shown that stellar rotation can change the strength of dynamical tide significantly. In particular, retrograde rotation with respect to the orbit increases the energy transfer by bringing lower-order g-modes (or f-mode for convective stars), which couple more strongly to the tidal potential, into closer resonances with the orbital motion of the companion.

We apply our general formalism to the problems of tidal capture binary formation and the orbital evolution of PSR J0045-7319/B-star binary. Stellar rotation changes the critical impact parameter for binary capture. Although the enhancement (by retrograde rotation) in the capture cross section is at most  $\sim 20\%$ , the probability that the captured system survives disruption/merging and therefore becomes a binary can be significantly larger. It is found that in order to explain the observed rapid orbital decay of the PSR J0045-7319 binary system, retrograde rotation in the B-star is required.

*Subject headings:* binaries: close – pulsars: individual (PSR J0045-7319) – stars: neutron – stars: oscillations – stars: rotation – hydrodynamics

## 1. Introduction

The standard weak friction theory for tidal interaction in binary stars, first introduced by Darwin (1879), and developed in detail by many authors (e.g., Alexander 1973; Kopal 1978; Hut 1981), is based on the assumption of static tide in hydrostatic equilibrium. In the presence of finite dissipation, a tidal lag develops between the tidal bulge and the external tidal potential, and the resulting tidal torque drives the spin and orbital evolution. This theory has been applied successfully to planet-satellite systems (e.g., Goldreich & Peale 1968), and can also be used to describe binaries of low-mass (late-type) stars if appropriate turbulent viscosity due to convective eddies is used (Zahn 1977; Goodman & Oh 1997). The static tide approximation, however, is not appropriate for many other binary processes, especially those involving massive (early-type) stars with radiative envelopes, where dynamical excitation and radiative damping of low-frequency g-modes dominate the tidal interaction (Zahn 1977; Goldreich & Nicholson 1989). In these early works, the effect of rotation on the dynamical tide is neglected or introduced phenomenologically (but see Nicholson 1979 and Rocca 1989, where some aspects of rotational effects are explored), and only circular (or near circular) binary orbits are considered.

In this paper we study dynamical tides in rotating, eccentric binary stars. Our work is motivated by the recent observations of the PSR J0045-7319/B-star binary (Kaspi et al. 1996), which contains a radio pulsar and a massive rapidly-rotating B-star in an eccentric 51 days orbit, with periastron separation of only 4 stellar radii. This system therefore constitutes an excellent laboratory for studying dynamical tidal interaction. In a preliminary analysis (Lai 1996) of the rapid orbital decay of the binary as revealed by timing observation (Kaspi et al. 1996), it was realized that rotation can have rather significant effect on the strength of dynamical tides. In particular, when the B-star has a retrograde rotation (with magnitude of one half of the maximum value, for example) with respect to the orbital motion, the dynamical tidal energy is increased over the nonrotating value by two orders of magnitude. Roughly speaking, this comes about because retrograde rotation shifts the tidal resonance (where the mode frequency equals the external driving frequency) from high-order g-modes to lower-order ones, which couple much more strongly to the tidal potential. It is this enhancement of dynamical tide by retrograde rotation that allows the binary orbit to decay on a short time scale of 0.5 Myr, although it has been suggested (correctly in our opinion) by Kumar and Quataert (1997; hereafter KQ) that differential rotation is also required in order to keep the mode damping time relatively short (see §6 for more discussion). In this paper we present a full analysis of dynamical tides in rotating stars, with applications to the orbital evolution of the PSR J0045-7319/B-star binary. We shall focus on the dynamical aspects of the problem, i.e., those aspects that are independent of dissipation mechanisms. We particularly emphasize the difficulty with the usual mode decomposition because of the asymmetry between modes with opposite signs of pattern speed. Such difficulty has led to quantitatively misleading results concerning the tidal energy in stars with rapid prograde rotation (KQ; see §6.3 for discussion).

Another prominent example in which dynamical tides play an important role is binary

formation from tidal capture. This process was originally suggested by Fabian, Pringle & Rees (1975) to explain the origin of low-mass X-ray binaries in globular clusters: During a close passage of two stars in an unbound orbit, the excess orbital energy is transferred through dynamical tidal excitation to the internal stellar oscillations, resulting in a bound system. Although it has been recognized in recent years that primordial binaries play an important role in the dynamics of globular clusters, and may also be involved (via exchange interaction with another star) to produce low-mass X-ray binaries and other stellar exotica (e.g., Hut et al. 1992; Davies 1996), tidal capture can still be an efficient means to produce tight binaries, thereby providing an energy source to reverse core collapse. Many theoretical issues related to tidal capture process have been studied, including linear and nonlinear energy transfer (Press and Teukolsky 1977, hereafter PT; Lee & Ostriker 1986; Khokhlov, Novikov & Pethick 1993), evolution of the binary subsequent to capture (Kochanek 1992; Novikov, Pethick & Polnarev 1992; Mardling 1995) and dissipation of tidally excited modes (Kumar & Goodman 1996). However, the possible role of stellar rotation on the tidal energy and angular momentum transfer has not been considered. Indeed, we find in this paper that rotation changes the cross-section for tidal capture, and can significantly increase the probability of forming binaries through tidal interaction.

Our paper is organized as follows. In §2 we present the basic equations describing the tidal excitations of normal modes in a rotating star and the orbital response to the excited oscillations. We then derive in §3 general expressions for energy transfer and angular momentum transfer in a periastron passage when there is no initial oscillation. For an eccentric system, this energy transfer is directly proportional to the steady-state mode energy in the presence of dissipation, and provide a measure of the strength of the dynamical tide (see §6.1). In §4 we examine the properties of rotating modes that are relevant for tidal excitation; these are used in specific calculations presented in §§5-6. We apply our general formalism to the tidal capture problem in §5 and the orbital evolution of PSR J0045-7319/B-star binary in §6. A brief discussion of related problems is given in §7.

## 2. Basic Equations

Consider a rotating star with mass  $M$ , radius  $R$  and spin  $\mathbf{\Omega}_s$ , interacting with a companion  $M'$ . We treat  $M'$  as a point mass, although generalization to the case where both stars have finite structure is straightforward. For simplicity here we assume the spin axis is perpendicular to the orbital plane (but  $\Omega_s$  can have both positive and negative signs, corresponding to prograde and retrograde rotations with respect to the orbit). Generalized equations for arbitrary spin-orbit inclination angles are summarized in Appendix A.

In the linear regime, the perturbation of the tidal potential on  $M$  is specified by the Lagrangian displacement  $\tilde{\xi}(\mathbf{r}, t)$  of a fluid element from its unperturbed position. In the inertial

frame, the equation of motion can be written in the form: <sup>1</sup>

$$\frac{\partial^2}{\partial t^2} \vec{\xi} + 2(\mathbf{v} \cdot \nabla) \frac{\partial \vec{\xi}}{\partial t} + \mathbf{C} \cdot \vec{\xi} = -\nabla U, \quad (1)$$

where  $\mathbf{v} = \Omega_s \times \mathbf{r}$  is the unperturbed fluid velocity,  $\mathbf{C}$  is a self-adjoint operator (see Lyden-bell & Ostriker 1967). The external potential in Eq. (1) is given by

$$U(\mathbf{r}, t) = -\frac{GM'}{|\mathbf{r} - \mathbf{D}(t)|} = -GM' \sum_{lm} W_{lm} \frac{r^l}{D^{l+1}} \exp(-im\Phi) Y_{lm}(\theta, \phi), \quad (2)$$

where we have chosen a spherical coordinate system centered at  $M$  with the  $z$ -axis long the rotation axis and the  $x$ -axis pointing to the periastron:  $\mathbf{r}$  is the position vector of a fluid element the star, and  $\mathbf{D}(t) = [D(t), \pi/2, \Phi(t)]$  specifies the position of the point mass  $M'$  [ $D(t)$  is the orbital separation,  $\Phi(t)$  is the orbital phase], and  $W_{lm}$  is a coefficient as defined in PT:

$$W_{lm} = (-)^{(l+m)/2} \left[ \frac{4\pi}{2l+1} (l+m)!(l-m)! \right]^{1/2} \left[ 2^l \left( \frac{l+m}{2} \right)! \left( \frac{l-m}{2} \right)! \right]^{-1}, \quad (3)$$

[here the symbol  $(-)^k$  is to be interpreted as zero when  $k$  is not an integer]. In equation (2), the  $l = 0$  and  $l = 1$  terms should be dropped, since they are not relevant to tidal deformation. For  $l = 2$ , the only nonzero  $W_{lm}$ 's are  $W_{2\pm 2} = (3\pi/10)^{1/2}$  and  $W_{20} = -(\pi/5)^{1/2}$ , reflecting the symmetry of the tidal potential with respect to  $\phi \rightarrow \phi + \pi$ . Thus only modes with  $m = 0, \pm 2$  are excited.

An eigenmode  $\vec{\xi}_\alpha(\mathbf{r}, t) = \vec{\xi}_\alpha(\mathbf{r}) e^{i\sigma_\alpha t} \propto e^{i\sigma_\alpha t + im\phi}$  satisfies the equation

$$-\sigma_\alpha^2 \vec{\xi}_\alpha + 2i\sigma_\alpha (\mathbf{v} \cdot \nabla) \vec{\xi}_\alpha + \mathbf{C} \cdot \vec{\xi}_\alpha = 0, \quad (4)$$

where  $\sigma_\alpha$  is the mode angular frequency in the inertial frame, and  $\alpha = \{n jm\}$  specifies the mode index:  $n$  gives the number of nodes in the radial eigenfunction (the order of the mode),  $j$  specifies the number of nodes in the  $\theta$ -eigenfunction ( $j$  reduces to  $l$  in the nonrotating limit), and  $m$  is the azimuthal mode index. We shall use the convention  $\sigma_\alpha > 0$  in this paper, so that a  $m > 0$  mode has a retrograde pattern speed ( $-\sigma/m < 0$ ), while a  $m < 0$  mode has a prograde pattern speed. Although the normal modes are not complete in strict mathematical sense, any reasonable initial data for Eq. (1) evolve in time as a linear superposition of the eigenmodes  $\vec{\xi}_\alpha(\mathbf{r})$  (see Dyson & Schutz 1979 for an analysis of the completeness problem). Thus we write  $\vec{\xi}(\mathbf{r}, t) = \sum_\alpha a_\alpha(t) \vec{\xi}_\alpha(\mathbf{r})$ , and normalize the eigenmode via  $\int d^3x \rho \vec{\xi}_\alpha \cdot \vec{\xi}_\alpha = 1$ . Substituting this expansion into Eq. (1) and using Eq. (4), we obtain the dynamical equation for the mode amplitude:

$$\ddot{a}_\alpha + \sigma_\alpha^2 a_\alpha - 2iB_\alpha(\dot{a}_\alpha - i\sigma_\alpha a_\alpha) + 2\gamma_\alpha \dot{a}_\alpha = \sum_l \frac{GM' W_{lm} Q_{\alpha l}}{D^{l+1}} e^{-im\Phi}, \quad (5)$$

---

<sup>1</sup>The mode amplitude can be equivalently studied in the rotating frame. In this case, the equation of motion is  $\partial^2 \vec{\xi} / \partial t^2 + 2\Omega_s \times (\partial \vec{\xi} / \partial t) + \mathbf{C}' \cdot \vec{\xi} = -\nabla U$ , and in Eq. (2) we should replace  $\Phi$  by  $(\Phi - \Omega_s t)$ . Our treatment in the inertial frame is more convenient for generalization to the case of arbitrary spin-orbit inclination angles (Appendix A).

where  $Q_{\alpha l}$  is the tidal coupling coefficient (the overlap integral) defined by

$$Q_{\alpha l} = \int d^3x \rho \vec{\xi}_\alpha^* \cdot \nabla (r^l Y_{lm}) = \int d^3x \delta \rho_\alpha^* (r^l Y_{lm}), \quad (6)$$

[here  $\delta \rho_\alpha = -\nabla \cdot (\rho \vec{\xi}_\alpha)$  is the Eulerian density perturbation], and the function  $B_\alpha$  is given by

$$B_\alpha = i \int d^3x \rho \vec{\xi}_\alpha^* \cdot (\mathbf{v} \cdot \nabla) \vec{\xi}_\alpha = -m\Omega_s + i \int d^3x \rho \vec{\xi}_\alpha^* \cdot (\mathbf{\Omega}_s \times \vec{\xi}_\alpha). \quad (7)$$

Note that  $\rho \vec{\xi}_\alpha^* \cdot (\mathbf{v} \cdot \nabla) \vec{\xi}_\alpha = \nabla \cdot (\rho \mathbf{v} |\vec{\xi}_\alpha|^2) - |\vec{\xi}_\alpha|^2 \nabla \cdot (\rho \mathbf{v}) - \rho \vec{\xi}_\alpha \cdot (\mathbf{v} \cdot \nabla) \vec{\xi}_\alpha^*$ , and one can easily show that  $B_\alpha$  is real. In deriving Eq. (5), we have assumed that different modes are orthogonal to each other, and have neglected the off-diagonal terms  $B_{\alpha\beta} \equiv i \int d^3x \rho \vec{\xi}_\beta^* \cdot (\mathbf{v} \cdot \nabla) \vec{\xi}_\alpha$ . This *approximation* allows us to decompose  $\vec{\xi}(\mathbf{r}, t)$  into normal modes and obtain a simple equation for individual mode amplitude. The limitation of this approximation will be examined in the next section [see the discussion following Eq. (28)].

We have also introduced in Eq. (5) the quantity  $\gamma_\alpha$ , which is proportional to the mode damping rate. Multiply Eq. (5) by  $\dot{a}_\alpha^*$  and take the real part, we find:

$$\frac{dE_\alpha}{dt} = -2\gamma_\alpha |\dot{a}_\alpha|^2 + \sum_l \frac{GM' W_{lm} Q_{\alpha l}}{D^{l+1}} \dot{a}_\alpha^* e^{-im\Phi}, \quad (8)$$

where the mode energy is given by <sup>2</sup>

$$E_\alpha = \frac{1}{2} |\dot{a}_\alpha|^2 + \frac{1}{2} (\sigma_\alpha^2 - 2B_\alpha \sigma_\alpha) |a_\alpha|^2. \quad (9)$$

The last term in Eq. (8) gives the rate at which energy is transferred to each mode. For free oscillation (without external driving),  $a_\alpha \propto e^{i\sigma_\alpha t}$ , the mode energy becomes  $\sigma_\alpha (\sigma_\alpha - B_\alpha) |a_\alpha|^2$ , and Eq. (8) reduces to  $dE_\alpha/dt = -2\Gamma_\alpha E_\alpha$ , with the mode amplitude damping rate given by

$$\Gamma_\alpha = \frac{\sigma_\alpha \gamma_\alpha}{\sigma_\alpha - B_\alpha}. \quad (10)$$

The excited modes affect the orbital motion through the tidal interaction potential

$$V_{\text{tide}} = -GM' \int d^3x \frac{\delta \rho(\mathbf{r}, t)}{|\mathbf{D} - \mathbf{r}|} = - \sum_{\alpha l} \frac{GM' W_{lm} Q_{\alpha l}}{D^{l+1}} a_\alpha(t) e^{im\Phi}. \quad (11)$$

Thus the equations of motion for the orbit are

$$\mu \ddot{D} = \mu D \dot{\Phi}^2 - \frac{MM'}{D^2} - \sum_{\alpha l} (l+1) \frac{GM' W_{lm} Q_{\alpha l}}{D^{l+2}} e^{im\Phi} a_\alpha(t), \quad (12)$$

$$\frac{d(\mu D^2 \dot{\Phi})}{dt} = \sum_{\alpha l} im \frac{GM' W_{lm} Q_{\alpha l}}{D^{l+1}} e^{im\Phi} a_\alpha(t). \quad (13)$$

---

<sup>2</sup>The canonical energy associated with perturbation  $\vec{\xi}(\mathbf{r}, t)$  is generally given by  $E_c = (1/2) \int d^3x \rho (|\partial \vec{\xi} / \partial t|^2 + \vec{\xi}^* \cdot \mathbf{C} \cdot \vec{\xi})$ . For  $\vec{\xi}(\mathbf{r}, t) = a_\alpha(t) \xi_\alpha(\mathbf{r})$ , the canonical energy reduces to Eq. (9).

Given the mode properties  $(\sigma_\alpha, Q_{\alpha l})$ , equations (5),(12) and (13) completely determine the time evolution of the tidally excited oscillations and the binary orbit. In general, the energy transfer between the star and the orbit in a periastron passage depends on the phases of the oscillation modes and thus varies from one orbit to another (e.g., Kochanek 1992; Mardling 1995). For a highly eccentric system (such as parabolic tidal capture and the PSR J0045-7319 binary, to be discussed in §5 and §6, respectively), an important measure of the strength of dynamical tide is the energy transfer to the star,  $\Delta E_s$ , and the corresponding angular momentum transfer,  $\Delta J_s$ , during the “first” periastron when there is no initial oscillation. General expressions for  $\Delta E_s$  and  $\Delta J_s$  are derived in the next section (§3). The relation between  $\Delta E_s$  and the steady-state tidal energy  $\langle E_s \rangle$  in elliptical binary system in the presence of dissipation is established in §6.1.

### 3. Energy Transfer and Angular Momentum transfer

Here we derive the expressions for the energy transfer  $\Delta E_s$  and angular momentum transfer  $\Delta J_s$  to the oscillation modes in a single periastron passage assuming the star has no initial oscillation. The binary orbit is characterized by the periastron distance  $D_p$  and two dimensionless quantities: the eccentricity  $e$ , and the ratio between the periastron passage time and the dynamical time of the star:

$$\eta = \left( \frac{M}{M_t} \right)^{1/2} \left( \frac{D_p}{R} \right)^{3/2} = (1 + e)^{1/2} \frac{1}{\hat{\Omega}_p}, \quad (14)$$

where  $M_t = M + M'$  is the total binary mass, and  $\hat{\Omega}_p$  is the orbital angular frequency at periastron in units of  $(GM/R^3)^{1/2}$ . We outline two derivations of  $\Delta E_s$  and  $\Delta J_s$ .

Our first derivation is patterned after PT. Since for very eccentric system, the orbital period is much longer than the timescale for periastron passage, and thus much longer than the periods of the tidally-excited normal modes, we can consider a continuous Fourier transform, viz.  $a_\alpha(t) = \int d\sigma e^{i\sigma t} \tilde{a}_\alpha(\sigma)$ . Equation (5) then becomes

$$(\sigma_\alpha^2 - \sigma^2) \tilde{a}_\alpha + 2B_\alpha(\sigma - \sigma_\alpha) \tilde{a}_\alpha + 2i\gamma_\alpha \sigma \tilde{a}_\alpha = \sum_l \frac{GM'}{D_p^{l+1}} Q_{\alpha l} K_{lm}(\sigma), \quad (15)$$

where  $K_{lm}(\sigma)$  depends on the orbital trajectory:

$$K_{lm}(\sigma) = \frac{W_{lm}}{2\pi} \int_{-\infty}^{\infty} dt \left( \frac{D_p}{D} \right)^{l+1} \exp(im\Phi + i\sigma t), \quad (16)$$

with the integration centered around the periastron (For elliptical orbit, the upper limit and lower limit of the integration should be replaced by  $P_{\text{orb}}/2$  and  $-P_{\text{orb}}/2$ ). The mode amplitude is then given by

$$a_\alpha(t) = \sum_l \int d\sigma e^{i\sigma t} \frac{GM' Q_{\alpha l} K_{lm}(\sigma)}{D_p^{l+1} [\sigma_\alpha^2 - \sigma^2 + 2B_\alpha(\sigma - \sigma_\alpha) + 2i\gamma_\alpha \sigma]}. \quad (17)$$

The energy transfer  $\Delta E_s$  to the oscillation modes (in the inertial frame) is obtained via

$$\Delta E_s = - \int dt \int d^3x \rho \frac{\partial \vec{\xi}}{\partial t} \cdot \nabla U^* = \int dt \sum_{\alpha l} \frac{GM' W_{lm} Q_{\alpha l}}{D^{l+1}} e^{im\Phi} \dot{a}_{\alpha}(t), \quad (18)$$

(only the real part of the expression is meaningful). Using Eq. (17), this becomes

$$\Delta E_s = \sum_{\alpha l l'} \frac{(GM')^2 Q_{\alpha l} Q_{\alpha l'} W_{lm} W_{l'm}}{2\pi} \iint dt dt' \frac{e^{im\Phi(t)+im\Phi(t')}}{[D(t)]^{l+1} [D(t')]^{l'+1}} A_{\alpha}(t, t'), \quad (19)$$

where

$$A_{\alpha}(t, t') = \int d\sigma \frac{i\sigma e^{i\sigma(t+t')}}{\sigma_{\alpha}^2 - \sigma^2 - 2B_{\alpha}(\sigma_{\alpha} - \sigma) + 2i\gamma_{\alpha}\sigma}. \quad (20)$$

This integral can be easily evaluated using a contour in the complex plane, yielding

$$A_{\alpha}(t, t') = \frac{\pi}{\sigma_{\alpha} - B_{\alpha}} \left[ \sigma_{\alpha} e^{i\sigma_{\alpha}(t+t')} + (\sigma_{\alpha} - 2B_{\alpha}) e^{-i(\sigma-2B_{\alpha})(t+t')} \right], \quad (21)$$

for  $t + t' > 0$ , and  $A_{\alpha}(t, t') = 0$  for  $t + t' < 0$ . The energy transfer is therefore

$$\Delta E_s = \frac{GM'^2}{R} \sum_{ll'} \left( \frac{R}{D_p} \right)^{l+l'+2} T_{ll'}(\eta, e), \quad (22)$$

with

$$T_{ll'}(\eta, e) = \pi^2 \sum_{\alpha} \frac{Q_{\alpha l} Q_{\alpha l'}}{\sigma_{\alpha} - B_{\alpha}} [\sigma_{\alpha} K_{lm}(\sigma_{\alpha}) K_{l'm}(\sigma_{\alpha}) + (\sigma_{\alpha} - 2B_{\alpha}) K_{l-m}(\sigma_{\alpha} - 2B_{\alpha}) K_{l'-m}(\sigma_{\alpha} - 2B_{\alpha})]. \quad (23)$$

In writing Eq. (22), we have factored out all dimensional physical quantities so that  $T_{ll'}$  is dimensionless, i.e., all quantities in  $T_{ll'}$  are in units such that  $G = M = R = 1$ . The angular momentum transfer is obtained via

$$\Delta J_s = \int dt \int d^3x \delta\rho \left( -\frac{\partial U^*}{\partial \phi} \right) = \int dt \sum_{\alpha l} (-im) \frac{GM' W_{lm} Q_{\alpha l}}{D^{l+1}} e^{im\Phi} a_{\alpha}(t). \quad (24)$$

Using a similar procedure we find:

$$\Delta J_s = \frac{GM'^2}{R} \left( \frac{R^3}{GM} \right)^{1/2} \sum_{ll'} \left( \frac{R}{D_p} \right)^{l+l'+2} S_{ll'}(\eta, e), \quad (25)$$

with

$$S_{ll'}(\eta, e) = \pi^2 \sum_{\alpha} \frac{Q_{\alpha l} Q_{\alpha l'}(-m)}{\sigma_{\alpha} - B_{\alpha}} [K_{lm}(\sigma_{\alpha}) K_{l'm}(\sigma_{\alpha}) - K_{l-m}(\sigma_{\alpha} - 2B_{\alpha}) K_{l'-m}(\sigma_{\alpha} - 2B_{\alpha})]. \quad (26)$$

For a given  $\alpha = \{n jm\}$ , the first terms inside the square brackets of Eq. (23) and Eq. (26) correspond to a mode with frequency  $\sigma_{\alpha}$ , while the second terms correspond to a mode with

frequency  $-(\sigma_\alpha - 2B_\alpha)$ . To see this more clearly, consider another derivation of  $\Delta E_s$  and  $\Delta J_s$ . We simply integrate Eq. (5) directly to obtain  $a_\alpha(t)$ :

$$a_\alpha(t) = \sum_l \frac{GM'W_{lm}Q_{\alpha l}}{2i(\sigma_\alpha - B_\alpha)} \left[ e^{i\sigma_\alpha t} \int_{-\infty}^t dt' \frac{e^{-im\Phi(t')-i\sigma_\alpha t'}}{D^{l+1}(t')} - e^{-i(\sigma_\alpha - 2B_\alpha)t} \int_{-\infty}^t dt' \frac{e^{-im\Phi(t')+i(\sigma_\alpha - 2B_\alpha)t'}}{D^{l+1}(t')} \right], \quad (27)$$

where we have neglected the damping term by setting  $\Gamma_\alpha = 0$ . Suppose the periastron passage occurs at  $t = 0$ , then for  $t \gg 0$ , we have

$$a_\alpha(t) = \sum_l \frac{\pi GM'Q_{\alpha l}}{iD_p^{l+1}(\sigma_\alpha - B_\alpha)} \left[ e^{i\sigma_\alpha t} K_{lm}(\sigma_\alpha) - e^{-i(\sigma_\alpha - 2B_\alpha)t} K_{l-m}(\sigma_\alpha - 2B_\alpha) \right]. \quad (28)$$

Using Eq. (9) we find that the total mode energy after the periastron passage is again given by Eqs. (22)-(23).

Equation (28) clearly reveals that after excitation in a periastron passage, a mode  $\vec{\xi}(r, \theta)e^{im\phi}$  oscillates at frequencies  $\sigma_\alpha$  (its eigenfrequency) and  $-(\sigma_\alpha - 2B_\alpha)$ . How can a mode oscillate at a frequency other than its own eigenfrequency? This conundrum comes from our approximate treatment of mode decomposition leading to Eq. (5). Note that the mode  $\vec{\xi}_\alpha \propto e^{-i\sigma t - im\phi}$  is physically identical to the mode  $\vec{\xi}_\alpha \propto e^{i\sigma t + im\phi}$ . For a given  $n, j$  and  $|m| = 2$  (for example), there are four mathematically distinct modes:<sup>3</sup>

$$\vec{\xi}_m(\mathbf{r}, t) = \vec{\xi}_2(r, \theta)e^{i2\phi + i\sigma_2 t}, \quad \vec{\xi}'_2(r, \theta)e^{-i2\phi - i\sigma_2 t}, \quad (\text{retrograde mode}); \quad (29)$$

$$\vec{\xi}_m(\mathbf{r}, t) = \vec{\xi}_{-2}(r, \theta)e^{-i2\phi + i\sigma_{-2} t}, \quad \vec{\xi}'_{-2}(r, \theta)e^{i2\phi - i\sigma_{-2} t}, \quad (\text{prograde mode}), \quad (30)$$

and only two of them are physically distinct, one with prograde pattern speed and another with retrograde pattern speed. Clearly, within the context of our approximation, we should identify  $(\sigma_m - 2B_m)$  with  $\sigma_{-m}$  (where the other mode indices  $n, j$  are suppressed). This  $(-\sigma_{-m})$  mode has wavefunction  $\vec{\xi}'_{-m}(r, \theta)$ , different from  $\vec{\xi}_m(r, \theta)$ , and thus its amplitude should be proportional to  $Q_{-m}$  rather than  $Q_m$  as indicated in Eq. (28). But this is an artifact of our approximation. In the slow rotation limit ( $|\Omega_s| \ll \sigma_\alpha$ ), the mode frequencies are related to the nonrotating value  $\sigma^{(0)}$  by  $\sigma_m = \sigma^{(0)} + B_m$  and  $\sigma_{-m} = \sigma^{(0)} + B_{-m} = \sigma^{(0)} - B_m$ , while the wavefunctions are unchanged to the leading order (so that  $Q_m = Q_{-m} = Q^{(0)}$ ). Thus Eqs. (22), (23), (25), (26) and (28) are exact in this limit. For larger rotation rates, they should still be good approximations as long as  $\sigma_m - 2B_m$  is close to  $\sigma_{-m}$ , and the difference between  $Q_m$  and  $Q_{-m}$  is small — We find that these are satisfied for the relevant modes considered in §5 and §6.

The preceding discussion leads us to adopt the following *ansatz*: The amplitude of each mode (specified by  $\alpha = \{n, j, m\}$  and the direction of pattern speed) is given by the first term of Eq. (27), while the contribution of the second term to  $\Delta J_s$  and  $\Delta E_s$  is identical to that of a corresponding

---

<sup>3</sup>It can be shown that if  $\vec{\xi}(r, \theta)e^{im\phi + i\sigma t}$  is a solution of Eq. (4), then  $\vec{\xi}'(r, \theta)e^{-im\phi - i\sigma t}$  is also a solution, where  $\vec{\xi}' = (\xi_r, \xi_\theta, -\xi_\phi)$ . These two modes have the same  $\delta\rho(r, \theta)$ . See Schutz (1979).

( $-m$ ) mode with the same pattern speed. The dimensionless energy transfer  $T$  and angular momentum transfer  $S$  are therefore given by

$$T_{ll'}(\eta, e) = 2\pi^2 \sum_{\alpha} \frac{Q_{\alpha l} Q_{\alpha l'}}{\sigma_{\alpha} - B_{\alpha}} \sigma_{\alpha} K_{lm}(\sigma_{\alpha}) K_{l'm}(\sigma_{\alpha}), \quad (31)$$

$$S_{ll'}(\eta, e) = 2\pi^2 \sum_{\alpha} \frac{Q_{\alpha l} Q_{\alpha l'}(-m)}{\sigma_{\alpha} - B_{\alpha}} K_{lm}(\sigma_{\alpha}) K_{l'm}(\sigma_{\alpha}),, \quad (32)$$

where the factor of 2 results from the equivalence of the  $(m, \sigma_{\alpha})$  mode and the  $(-m, -\sigma_{\alpha})$  mode. Since the mode pattern speed is  $(-\sigma_{\alpha}/m)$ , the contribution of each mode to the energy transfer  $\Delta E_{\alpha}$  and angular momentum transfer  $\Delta J_{\alpha}$  are related by  $\Delta J_{\alpha} = (-m/\sigma_{\alpha})\Delta E_{\alpha}$ , as seen from Eqs. (31) and (32). It is also useful to consider the total mode energy  $\Delta E_s^{(r)}$  in the star's rotating frame. Since the rotational kinetic energy associated with the angular momentum transfer is  $\Omega_s \Delta J_s$ , we have  $\Delta E_s^{(r)} = \Delta E_s - \Omega_s \Delta J_s$ , and the corresponding dimensionless energy is

$$T_{ll'}^{(r)}(\eta, e) = T_{ll'}(\eta, e) - \Omega_s S_{ll'}(\eta, e) = 2\pi^2 \sum_{\alpha} \frac{Q_{\alpha l} Q_{\alpha l'}}{\sigma_{\alpha} - B_{\alpha}} \omega_{\alpha} K_{lm}(\sigma_{\alpha}) K_{l'm}(\sigma_{\alpha}), \quad (33)$$

where  $\omega_{\alpha} = \sigma_{\alpha} + m\Omega_s$  is the mode frequency in the rotating frame. We emphasize that, although our procedure leading to Eqs. (31)-(33) is somewhat ad-hoc mathematically [The “rigorous” derivation of Eqs. (23), (26) and (28) are exact only in the slow-rotation limit], the forms of these expressions are naturally expected on the physical ground: the retrograde mode should be related to  $|Q_2 K_{l2}(\sigma_2)|^2$  and the prograde mode to  $|Q_{-2} K_{l-2}(\sigma_{-2})|^2$ . The only uncertainty is the factor  $(\sigma_{\alpha} - B_{\alpha})/\omega_{\alpha} = 1 - (i/\omega_{\alpha}) \int d^3x \rho \vec{\xi}_{\alpha}^* \cdot (\vec{\Omega}_s \times \vec{\xi}_{\alpha})$  [cf. Eq. (33)] which only serves as a insignificant “correction” to  $Q_{\alpha}$  (see §6 for further discussion).

Although the above expressions apply for general  $l$ , in this paper we shall consider only the quadrupolar ( $l = 2$ ) tides. The contribution of higher- $l$  tidal potential to  $\Delta E_s$  is of order  $(R/D_p)^2$  smaller than that of the leading  $l = 2$  term.

#### 4. Properties of Modes in Rotating Stars

We consider two simple stellar models in this paper: (i) A  $\Gamma = \Gamma_1 = 5/3$  polytrope ( $\Gamma$  is the polytropic index,  $\Gamma_1$  is the adiabatic index), representing low-mass ( $M \lesssim 0.5M_{\odot}$ ) MS star with thick convective envelope; (ii) A  $\Gamma = 4/3$ ,  $\Gamma_1 = 5/3$  polytrope, representing high-mass (larger than a few solar mass) star for which the envelope is radiative; it is also a good approximation to the outer structure of intermediate-mass stars ( $\sim 1M_{\odot}$ ).

We examine the effects of rotation on the mode properties (frequency and tidal coupling coefficient) relevant to tidal excitation.

#### 4.1. f-Mode and p-Modes

For low-mass, convective star (which does not have any g-mode), the f-mode and lowest order p-modes are the most important modes that absorb tidal energy. For  $\Omega_s$  much smaller than the mode frequency, perturbation theory is adequate (e.g., Unno et al. 1989). To leading order, the mode wavefunction is unchanged, and the mode frequency is modified from the nonrotating value  $\sigma_{nl}^{(0)}$  by

$$\sigma_{nlm} = \sigma_{nl}^{(0)} + B_{nlm} = \sigma_{nl}^{(0)} - m\Omega_s + mC_{nl}\Omega_s, \quad (34)$$

where  $m\Omega_s C_{nl} = i \int d^3x \rho \vec{\xi}_\alpha^* \cdot (\vec{\Omega}_s \times \vec{\xi}_\alpha)$ . Using the zeroth order eigenfunction  $\vec{\xi}_{nlm}(\mathbf{r}) = [\xi_r(r)\mathbf{e}_r + \xi_\perp(r)\hat{\nabla}_\perp] Y_{lm}(\theta, \phi)$ , where  $\hat{\nabla} = \mathbf{e}_\theta(\partial/\partial\theta) + (\mathbf{e}_\phi/\sin\theta)(\partial/\partial\phi)$ , we have

$$C_{nl} = \int_0^R \rho r^2 (2\xi_r \xi_\perp + \xi_\perp^2) dr, \quad (35)$$

and the eigenfunction is normalized via  $\int d^3x \rho \vec{\xi}^* \cdot \vec{\xi} = \int dr \rho r^2 [\xi_r^2 + l(l+1)\xi_\perp^2] = 1$ . In the rotating frame the mode angular frequency is  $\omega_{nlm} = \omega_{nl}^{(0)} + mC_{nl}\Omega_s$ . For the  $\Gamma = 5/3$  polytrope, we have  $C_{02} = 0.4955$  (f mode),  $C_{12} = 0.1525$  (p<sub>1</sub> mode), and  $C_{22} = 0.0787$  (p<sub>2</sub> mode); for the  $\Gamma = 4/3$ ,  $\Gamma_1 = 5/3$  polytrope, we have  $C_{02} = 0.2543$  (f mode),  $C_{12} = 0.1538$  (p<sub>1</sub> mode), and  $C_{22} = 0.0818$  (p<sub>2</sub> mode). For higher  $\Omega_s$ , linear perturbation theory breaks down, but accurate numerical results are available (e.g., Managan 1986; Ipser & Lindblom 1990). The latter is essentially an exact method). In our calculation of tidal capture below (§5), we shall adopt the linear approximation at small  $\Omega_s$  with correction for high  $\Omega_s$  using the results given in Managan (1986). The modification to the mode eigenfunction is negligible and therefore we set  $Q_\alpha = Q_{\alpha 2}$  to be the same as that of a nonrotating star.

#### 4.2. g-Modes

For intermediate to massive stars with radiative envelopes, g-modes dominate the tidal energy transfer because their relatively low frequencies match the orbital frequency at periastron (see §§5-6). Since we shall consider the cases where the rotation frequency is comparable or larger than the g-mode frequency, the perturbation theory is not adequate. An approximate treatment of g-modes in rapidly rotating star is based on the so-called “traditional approximation” (Chapman & Lindzen 1970; Unno et al. 1989; Bildsten et al. 1996), where the centrifugal distortion of the star is neglected, as well as the Coriolis forces associated with the horizontal component of the spin angular velocity. Note that this approximation is strictly valid only for high-order g-modes for which  $\omega_\alpha \ll N$  (where  $N$  is the Brunt-Väisälä frequency) and  $\xi_\perp \gg \xi_r$ , and for  $\Omega_s \ll N$  (so that the radial component of the Coriolis force can be neglected compared to the buoyancy force), but it also provides a good estimate even for low-order modes.

Neglecting the perturbation in the gravitational potential (Cowling approximation) and adopting the traditional approximation, the radial Lagrangian displacement and Eulerian pressure

perturbation can be written as

$$\xi_r(\mathbf{r}) = \xi_r(r) H_{jm}(\theta) e^{im\phi}, \quad \delta P(\mathbf{r}) = \delta P(r) H_{jm}(\theta) e^{im\phi}, \quad (36)$$

where  $H_{jm}(\theta)$  is the Hough function, satisfying the Laplace tidal equation (Chapman & Lindzen 1970). Separating out the angular dependence, the fluid continuity equation and Euler equation (in the rotating frame) reduce to a set of coupled radial equations:

$$\frac{d}{dr} \delta P = -\frac{g}{c_s^2} \delta P + \rho(\omega^2 - N^2) \xi_r, \quad (37)$$

$$\frac{d}{dr} (r^2 \xi_r) = \frac{g}{c_s^2} (r^2 \xi_r) - \frac{r^2}{c_s^2 \rho} \delta P + \frac{\lambda}{\omega^2 \rho} \delta P, \quad (38)$$

where the mode index  $\alpha = \{n jm\}$  has been suppressed, and  $g > 0$  is the gravitational acceleration,  $c_s$  is the sound speed. The eigenvalue of the Laplace tidal equation,  $\lambda$ , depends on  $m$  and the ratio  $q = 2\Omega_s/\omega_\alpha$ . For  $q \rightarrow 0$  (nonrotating case), the function  $H_{jm}(\theta) e^{im\phi}$  becomes  $Y_{lm}(\theta, \phi)$  while  $\lambda$  degenerates into  $l(l+1)$ .

The properties of the Hough function have been extensively studied (Longuet-Higgins 1967). We have adopted the numerical approach of Bildsten et al. (1996) in our calculation. For given  $q$  and  $m$ , the eigenvalue  $\lambda$  is obtained by solving the angular equation. The radial equations (37)-(38) are then solved together with appropriate boundary conditions to obtain  $\omega$ , from which the actual rotation rate  $\Omega_s = q\omega/2$  is recovered. Figure 1 shows the frequencies (in the rotating frame) of several  $j = 2$  g-modes against the rotation rate (Both  $\omega$  and  $\Omega_s$  are plotted in units of  $\omega^{(0)}$ , the mode frequency at zero rotation). These modes have  $l = 2$  in the  $\Omega_s = 0$  limit. For high order g-modes, a WKB analysis for the radial equations gives  $\omega \propto \sqrt{\lambda}$ . Thus we have  $\omega/\omega^{(0)} = \sqrt{\lambda/6}$  and  $\Omega_s/\omega^{(0)} = q\sqrt{\lambda/24}$ . For  $|\Omega_s/\omega^{(0)}| < 1.1$  (which is satisfied by g-modes with  $n \leq 13$  when  $\Omega_s < 0.5$ ), our numerical results for the g-modes of the  $\Gamma = 4/3$ ,  $\Gamma_1 = 5/3$  polytrope can be fitted by the following analytic expressions to within 1%: <sup>4</sup>

$$\bar{\omega} = 1 + \left[ (1/3)\bar{\Omega}_s + (13/42)\bar{\Omega}_s^2 - 0.064\bar{\Omega}_s^{4.6} \right] f, \quad (m = 2), \quad (39)$$

$$\bar{\omega} = 1 + \left[ (6/7)\bar{\Omega}_s^2 - 0.31|\bar{\Omega}_s|^{3.3} \right] f, \quad (m = 0), \quad (40)$$

$$\bar{\omega} = 1 + \left[ -(1/3)\bar{\Omega}_s + (13/42)\bar{\Omega}_s^2 - 0.118\bar{\Omega}_s^3 \right] f, \quad (m = -2), \quad (41)$$

where  $\bar{\omega} \equiv \omega/\omega^{(0)}$ ,  $\bar{\Omega}_s \equiv \Omega_s/\omega^{(0)}$ , and the factor  $f \leq 1$  depends on specific g-modes: In the WKB limit (high-order g-modes with  $n \rightarrow \infty$ ) we have  $f = 1$ . The values of  $f$  for other selected modes are:  $f = 0.48, 0.81, 0.9, 0.95$  for  $g_1, g_5, g_{10}, g_{20}$ . Equations (39)-(41) break down when  $|\bar{\Omega}_s| \gtrsim 1.1$ . In this high- $\bar{\Omega}_s$  regime, the following asymptotic expressions can be applied:  $\bar{\omega} \simeq 1.54\sqrt{\bar{\Omega}_s}$  (for  $m = 0, 2$ ), and  $\bar{\omega} \simeq 0.82$  (for  $m = -2$ ). Note that these expressions

<sup>4</sup> In these expressions, the linear and quadratic terms are derived from an analytic expansion of  $\lambda$  for small  $q$  (Bildsten & Ushomirsky 1996, private communication), and the last terms are based on numerical fitting.

[Eqs. (39)-(41)] are valid only for  $\Omega_s \geq 0$ . The eigenfrequencies for  $\Omega_s < 0$  can be obtained using the relation  $\omega_m(\Omega_s) = \omega_{-m}(-\Omega_s)$ .

Rotation also changes the tidal coupling coefficient  $Q_{\alpha 2}$ , although the correction is not significant since all the g-modes we include in our calculation ( $n \leq 20$ ) that are strongly excited satisfy  $\Omega_s/\omega^{(0)} < 1.7$ , i.e.,  $\Omega_s$  is not much larger than the mode frequency. Expressions for evaluating the  $Q_{\alpha l}$  and  $B_{\alpha}$  are given in Appendix B. Figure 2 shows the coupling coefficient  $Q_{\alpha} = Q_{\alpha 2}$  for several g-modes.

For rotating stars, the  $j = 4, 6, 8, \dots$  (corresponding to  $l = 4, 6, 8, \dots$  in the  $\Omega_s \rightarrow 0$  limit) modes with  $m = 0, \pm 2$  are also coupled to the quadrupolar tidal potential. (The coupling with the  $j = 3, 5, 7, \dots$  modes vanishes because the eigenfunctions are odd with respect to the equator while the tidal potential is even). The coupling goes to zero at  $\Omega_s = 0$ . Some properties of the  $j = 4$  modes are plotted in Figure 3 and compared with the  $j = 2$  modes. Two factors make these higher- $j$  modes less important to energy transfer during a tidal encounter than the  $j = 2$  modes: (i) The  $j \geq 4$  modes have higher frequencies than the  $j = 2$  modes of the same radial order, therefore resonance condition (see next section) is satisfied for higher-order modes, which couple less strongly to the tidal potential; (ii) The  $j \geq 4$  modes have much smaller coupling coefficients than the  $j = 2$  modes of the same radial order (The angular integral  $Q_{\theta}$  is plotted in Fig. 3(b); the radial integral  $Q_r$  is slightly smaller for the  $j = 4$  modes than for the  $j = 2$  modes). We have checked that the contribution of the  $j > 2$  modes to the energy transfer is always less than a few percent. Thus they are neglected in our calculations below.

### 4.3. r-Modes

For nonrotating stars, these are “trivial” toroidal modes with zero frequency and zero density perturbation, and thus they do not couple to the tidal potential. With rotation these modes are mixed with spheroidal components, and attain finite frequencies. The r-mode (sometimes also called “quasi-toroidal mode”) is the generalized form of Rossby waves on a spherical surface as studied in terrestrial meteorology. For small rotation rate  $|\Omega_s| \ll 1$ , r-modes can be studied using perturbation expansion in powers of  $\Omega_s$  (Provost et al. 1981; Saio 1982). To linear order in  $\Omega_s$ , the mode frequency increases as  $\omega = 2m\Omega_s/l(l+1)$ , while its Lagrangian displacement remains purely toroidal. Finite density perturbation comes in only in the second order of  $\Omega_s$ . For higher  $\Omega_s$ , r-modes can also be associated with eigenvalues of the Laplace tidal equation (Longuet-Higgins 1967). Since the coupling between r-modes and the tidal potential is weak ( $Q_{\alpha} \propto \Omega_s^2$ ), we shall neglect them in our calculations below.

## 5. Tidal Capture Binary Formation

We now apply the results of §§3-4 to study the effect of rotation on tidal capture. As long as the relative velocity between the stars at infinite separation is much less than the escape velocity from the star, a parabolic orbit is a good approximation. We consider two representative stellar models in §5.1 and §5.2.

### 5.1. Intermediate to Massive Stars: $\Gamma = 4/3$ Polytrope

For the  $\Gamma = 4/3$ ,  $\Gamma_1 = 5/3$  polytrope, the functions  $T_2^{(r)} = T_{22}^{(r)}$ ,  $S_2 = S_{22}$  and  $T_2 = T_2^{(r)} + \Omega_s S_2$  [where  $\Omega_s$  is the rotation rate in units of  $(GM/R^3)^{1/2}$ ] are plotted against  $\eta$  in Figure 4 for  $\Omega_s = 0, \pm 0.2$  and  $\pm 0.4$ . We clearly see that for  $\Omega_s < 0$  (retrograde rotation), the energy and angular momentum transfers can be significantly increased over the nonrotating values. This comes about for the following reasons: During a perastron passage, the most strongly excited modes are those (i) propagating in the same direction as the orbital motion of the companion (corresponding to the  $m = -2$  modes in our notation), (ii) having frequencies in the inertial frame comparable to the “driving frequency”, which is equal to twice of orbital frequency at periastron, i.e.,  $\sigma_\alpha = \omega_\alpha - m\Omega_s = 2\Omega_p$  (the “resonant condition”), and (iii) having relatively large  $Q_\alpha$ . Since higher-order (lower frequency) g-modes have smaller coupling coefficients than the low-order ones, the trade-off between (ii) and (iii) implies that the modes that absorb most tidal energy are those with frequencies higher than the resonant mode. For example, when  $\eta = 7$  and  $\Omega_s = 0$ , the resonant mode is  $g_{15}$ , with frequency  $\omega_\alpha \simeq 0.4 \simeq 2\Omega_p$ , while the dominant modes in energy transfer are  $g_6-g_8$  (which have  $\omega_\alpha = 0.85 - 0.68$ ). A retrograde rotation “drags” such  $m = -2$  waves backward, so that the mode frequencies in the inertial frame are lowered. As a result, the dominant modes in energy transfer are shifted to lower radial orders. Because  $Q_\alpha$  increases rapidly with decreasing mode order or increasing mode frequency (we find from numerical calculations that  $Q_\alpha \propto \omega_\alpha^{4.5}$  for nonrotating  $\Gamma = 4/3$  polytrope), the energy transfer is greatly increased. For example, at  $\Omega_s = -0.4$  and  $\eta = 7$ , the dominant modes are  $g_3-g_5$ , the net energy transfer (in the inertial frame)  $\Delta E_s$  is about 20 times larger than the nonrotating value.

While relatively small prograde rotation ( $\Omega_s > 0$ ) decreases the energy transfer, we see from Fig. 4 that for sufficiently large  $\Omega_s$  (or more precisely for sufficiently large ratio of  $\Omega_s/\Omega_p$ ),  $\Delta J_s$  or even  $\Delta E_s$  can become negative, i.e., angular momentum and energy are transferred from the star to the orbit (see also Fig. 8 in §6). This behavior can be understood as follows: The angular momentum of a mode is related to its energy in the rotating frame by  $J_\alpha = (-m/\omega_\alpha)E_\alpha^{(r)}$ , thus the prograde mode ( $m = -2$ ) carries positive angular momentum, while the retrograde mode carries negative angular momentum (Note that  $E_\alpha^{(r)}$  is always positive). For a fixed  $\eta$ , prograde rotation increases the frequencies of the prograde modes, shifts the resonance to higher radial orders (which have smaller  $Q_\alpha$ ), therefore decreases the positive angular momentum transfer to the star. On the other hand, the retrograde modes are “dragged” forward by the rotation, and their  $\sigma$ ’s become

smaller and may even become negative (i.e., they are prograde in the inertial frame). Therefore their contributions to the energy transfer become increasingly more important and the negative angular momentum transfer to the star increases as  $\Omega_s$  increases. When the negative angular momentum transferred to the  $m = 2$  modes becomes larger than the positive angular momentum transferred to the  $m = -2$  modes, the net  $\Delta J_s$  changes sign, and at the same time,  $\Delta E_s^{(r)}$  begins to increase with increasing  $\Omega_s$  (for a given  $\eta$ ). At even larger  $\Omega_s$ , when the change in the rotational energy  $\Omega_s \Delta J_s < 0$  (due to angular momentum lost to the orbit) dominates over the kinetic energy in the modes, the net  $\Delta E_s$  becomes negative. Our numerical results for the critical  $\Omega_s$  at which  $\Delta J_s$  or  $\Delta E_s$  changes sign can be fitted nicely by (for  $0.1 < \Omega_p < 0.35$ )

$$\Omega_s = 1.2\Omega_p + 0.08, \quad \text{for } \Delta J_s = 0 \quad (42)$$

$$\Omega_s = 1.5\Omega_p + 0.07, \quad \text{for } \Delta E_s = 0. \quad (43)$$

Kumar & Quataert (1997) claimed that  $\Delta J_s$  and  $\Delta E_s$  become negative when  $\Omega_s \gtrsim \Omega_p$ . This is different from our Eqs. (42)-(43). We believe this quantitative difference arises from their problematic treatment of mode decomposition. We defer a discussion of this point to the next section (§6.3).

The maximum  $D_p$  for capture is determined by the condition  $\Delta E^{(i)}(M) + \Delta E^{(i)}(M') = \mu v^2/2$ , where  $\Delta E^{(i)}(M) = \Delta E^{(i)}$  and  $\Delta E^{(i)}(M')$  are the energy transfer to  $M$  and  $M'$  respectively,  $\mu$  is the reduced mass and  $v$  is the relative velocity of the two stars at infinite separation. For  $1.8 \leq \eta \leq 3.5$  (the relevant parameter regime for capture) the function  $T_2$  can be fitted to the form

$$T_2 = T_2^{(r)} + \Omega_s S_2 = A \eta^{-\alpha}, \quad (44)$$

where the fitting parameters  $A$ ,  $\alpha$  for several  $\Omega_s$  are listed in Table 1. Let  $q = M'/M$  and  $\lambda = 1 + \Delta E^{(i)}(M')/\Delta E^{(i)}(M)$ , we then obtain the critical periastron distance for capture:

$$D_{\text{cap}} = R \left[ 2 \lambda A q (1 + q)^{(2+\alpha)/2} \right]^{2/3(4+\alpha)} \left[ \frac{v}{(GM/R)^{1/2}} \right]^{-4/3(4+\alpha)}. \quad (45)$$

Figure 5 depicts numerical results for the encounter between a  $1M_\odot$  star (modeled as a  $\Gamma = 4/3$ ,  $\Gamma_1 = 5/3$  polytrope) and a  $M' = 1.4M_\odot$  point mass (neutron star). With  $\lambda = 1$ , Equation (45) and Table 1 give  $D_{\text{cap}}/R = 2.42 v_{10}^{-0.188}$  for  $\Omega_s = 0$  [This agrees with Lee & Ostriker (1986)],  $D_{\text{cap}}/R = 2.10 v_{10}^{-0.136}$  for  $\Omega_s = 0.5$ , and  $D_{\text{cap}}/R = 2.77 v_{10}^{-0.230}$  for  $\Omega_s = -0.5$ , where  $v_{10} \equiv v/(10 \text{ km s}^{-1})$ .

## 5.2. Low Mass stars: $\Gamma = 5/3$ Polytrope

This is more applicable for low-mass (convective) stars (e.g., those in globular clusters). In this case, only the f-mode ( $\omega = 1.456$  for  $\Omega_s = 0$ ) is strongly excited, while the contribution of p-modes to the energy transfer is always less than a few percent because of their larger frequencies

and smaller  $Q_\alpha$  (e.g., for  $\Omega_s = 0$ , the  $p_1$  mode has  $\omega = 3.21$ , implying that it is almost always out of resonance, and its  $Q_\alpha$  is an order of magnitude smaller than that of the f-mode). We find similar rotational effect on energy transfer as in §5.1, although it is less prominent (since there is only one radial mode involved). For sufficiently large  $\Omega_s$ , the angular momentum transfer  $\Delta J_s$  changes signs, but this occurs only at  $\Omega_s/\Omega_p \gtrsim 3.5$ ; the energy transfer  $\Delta E_s$  never changes sign as long as we restrict to the regime  $\Omega_s < 0.6$  (i.e.,  $\Omega_s$  is less than the maximum rotation rate).

Motivated by the functional form of  $K_{lm}$  in the asymptotic limit ( $\eta\omega \gg 1$ ; see Appendix C), we can fit the function  $T_2$  to the form:

$$T_2 = T_2^{(r)} + \Omega_s S_2 = A \eta^5 \exp(-\alpha\eta), \quad (46)$$

with the fitting parameters  $A$  and  $\alpha$  given in Table 1. This fitting is valid for the range of  $\eta$  near tidal capture. In the asymptotic limit, including only the  $m = -2$  f-mode contribution, we have  $\alpha = 4\sqrt{2}\sigma/3$ . For  $\Omega_s = 0$ , this gives  $\alpha = 2.74$ . Figure 6 shows numerical results for encounter between a  $1M_\odot$  star (modeled as a  $\Gamma = 5/3$  polytrope) and a  $M' = 1.4M_\odot$  point mass (neutron star). Again, we see that the critical capture radius increases with increasing retrograde rotation.

### 5.3. Discussion on Tidal Capture Binary Formation

The results of §§5.1-5.2 indicate that stellar rotation can increase or decrease the critical capture radius by up to  $\sim 20\%$  (for nearly maximumly rotating stars), leading to similar change in the capture cross-section  $\sigma_{\text{cap}} \simeq 2\pi G(M + M')D_p/v^2$  (where  $v$  is the relative velocity of the stars in infinite separation). In globular clusters, the stellar rotation is likely to be much less than the maximum since the stars presumably have slowed down significantly by magnetic braking. For open clusters (with much lower velocity dispersion,  $\sim 1 \text{ km s}^{-1}$ ) or other young star clusters, such rapid rotation is certainly realistic (e.g., the typical surface rotation velocity for B stars is  $\sim 400 \text{ km/s}$ , corresponding to a rotation rate close to the maximum). While the 20% change in  $D_{\text{cap}}$  may seem insignificant by itself, we note that the enhancement to the probability for tidal capture binary formation can be much larger. Indeed, it has been suggested that almost all tidally captured bound systems may merge during the subsequent periastron passages, leaving no binaries behind (e.g., McMillan et al. 1987; Kochanek 1992). The critical periastron distance for merging,  $D_{\text{merge}}$ , is uncertain, but a reasonable lower limit is given by the sum of the radii of the two stars. Clearly, if  $D_{\text{merge}}$  is close to  $D_{\text{cap}}$ , then a relatively small increase in  $D_{\text{cap}}$  can lead to much larger increase in the efficiency for binary formation. If so, we can predict that *binaries formed by tidal capture must preferentially have retrograde rotations*. Although subsequent tidal evolution tends to align the spin and the orbital angular momentum, the retrograde signature may still be preserved for relatively young binaries.

## 6. Orbit and Spin Evolution of PSR J0045-7319/B-star Binary

The PSR J0045-7319 binary, containing a 0.93 s radio pulsar and a massive B-star companion ( $M = 8.8M_{\odot}$ ,  $R = 6.4R_{\odot}$ ) in an eccentric ( $e = 0.808$ ) 51.17 days orbit (Kaspi et al. 1994), is unique and important in that it is one of the two binary pulsars discovered so far that have massive main-sequence star companions (The other one is PSR B1259-63 with a Be-star companion; Johnston et al. 1994). These systems evolve from MS-MS binaries when one of the stars explode in a supernova to form a neutron star. Thus the characteristics of such pulsar binaries can potentially be used to infer the physical conditions of neutron star at its formation. The PSR J0045-7319 system, in particular, owing to its relatively small orbit and “clean” environment, exhibits two interesting dynamical orbital behaviors: (i) spin-orbit precessions due to the rapid, misaligned rotation of the B-star, which strongly suggests that the neutron star received a kick at birth from asymmetric supernova (Lai et al. 1995; Kaspi et al. 1996); (ii) Rapid orbital decay, on a timescale of  $P_{\text{orb}}/\dot{P}_{\text{orb}} = -0.5$  Myr (shorter than the lifetime of the  $8.8M_{\odot}$  B-star and the characteristic age of the pulsar) (Kaspi et al. 1996), which, together with a generic model of tidal evolution, can be used to constrain the age of the binary since the supernova and the initial spin of the pulsar (Lai 1996).

The mechanism for the orbital decay was discussed in Lai (1996). Since mass loss from the B-star is negligible (as inferred from dispersion measure variation; Kaspi et al. 1996b), the orbital decay must have a dynamical origin. The static tide, corresponding to the global, quadrupolar distortion of the star, cannot explain such rapid orbital decay because (i) it would require too short a viscous time (less than 30 days based on our numerical integrations of the tidal equations given by Alexander 1973) — Such a small viscous time is almost certainly impossible (e.g., even if the star were completely convective, the viscous time would still be longer than one year); (ii) It would lead to rapid spin-orbit synchronization and alignment even if viscosity were large enough to explain the observed  $\dot{P}_{\text{orb}}$ , in contradiction with observations. It was suggested that dynamical tidal interaction between the pulsar and the B-star can explain the rapid orbital decay provided that the B-star has significant retrograde rotation with respect to the orbital motion so that the energy transfer is sufficiently large. The reason that retrograde rotation significantly increases the tidal strength is the same as discussed in §5.1, i.e., retrograde rotation shifts the resonance from high-order g-modes to lower-order ones, which couple more strongly to the tidal potential. Several simplifying assumptions were adopted in the preliminary analysis of Lai (1996). The most important one is that the mode damping times are assumed to be constant since only small numbers of modes are strongly excited. This assumption is likely to be inadequate, as correctly pointed out by KQ, who suggested that an additional ingredient, differential rotation, is needed to compensate for the longer damping times of lower-order g-modes. Our focus here, however, is still to explore the dyanmcal aspects of the tides more completely.

### 6.1. Dynamical Tidal Energy: Steady State

The dynamical equations presented in §2 for the coupled orbital and mode evolution can be integrated numerically. Figure 7 depicts a typical example of such numerical integration. We start the calculation at the apastron ( $t_o = -P_{\text{orb}}/2$ ) with no initial oscillation, and include g-modes of order  $2 - 8$  (each has  $m = 0, \pm 2$  components). The total angular momentum  $J_{\text{trans}}$  and energy  $E_{\text{trans}}$  transferred to the modes are calculated via

$$J_{\text{trans}}(t) = \int_{t_o}^t dt \sum_{\alpha} \frac{GM'W_{lm}Q_{\alpha}}{D^{l+1}}(-im) a_{\alpha} e^{im\Phi}, \quad (47)$$

$$E_{\text{trans}}(t) = \int_{t_o}^t dt \sum_{\alpha} \frac{GM'W_{lm}Q_{\alpha}}{D^{l+1}} \dot{a}_{\alpha} e^{im\Phi}. \quad (48)$$

Obviously  $J_{\text{trans}}$  is equal to the mode angular momentum  $J_s$ , while  $E_{\text{trans}}$  is equal to the mode energy  $E_s = \sum_{\alpha} (1/2) [|\dot{a}_{\alpha}|^2 + (\sigma_{\alpha}^2 - 2B_{\alpha}\sigma_{\alpha})|a_{\alpha}|^2]$  only in the absence of dissipation ( $\Gamma_{\alpha} = 0$ ). We have checked that angular momentum conservation ( $J_s + J_{\text{orb}} = \text{const}$ ) and “energy conservation” ( $E_{\text{trans}} + E_{\text{orb}} = \text{const}$ ; of course the energy of the system,  $E_s + E_{\text{orb}}$ , is not conserved due to dissipation) are satisfied numerically to high accuracy.

Figure 7 reveals that, although initially the energy transfer during periastron passage varies from one orbit to another, after a few dissipation time, the mode energy  $\langle E_{\alpha} \rangle$  averaged over an orbit reaches a constant. In this steady state, the energy transferred to a mode at periastron is exactly balanced by the energy dissipated in one orbital period. Moreover, the mean mode energy  $\langle E_{\alpha} \rangle$  is approximately equal to the energy transfer in the first periastron passage,  $\Delta E_{\alpha}$ , which has been discussed in §3. This apparent coincidence can be understood as follows. Consider a mode with a given  $\alpha$  and sign of pattern speed. Its amplitude evolves according to the first term of Eq. (27), with the damping factor included:

$$a_{\alpha}(t) = \frac{GM'W_{lm}Q_{\alpha}}{2i(\sigma_{\alpha} - B_{\alpha})} e^{i\sigma_{\alpha}t - \Gamma_{\alpha}t} \int_{t_i}^t dt' \frac{e^{-im\Phi(t') - i\sigma_{\alpha}t' + \Gamma_{\alpha}t'}}{D^{l+1}(t')}. \quad (49)$$

Let  $t_j = (2j - 1)P_{\text{orb}}/2$  (with  $j = 0, 1, 2, \dots$ ) be the times at apastron. After the  $k$ -th periastron passage, the mode amplitude can be written as

$$a_{\alpha}(t_k) = (\Delta a_{\alpha}) e^{(i\sigma_{\alpha} - \Gamma_{\alpha})t_k} \sum_{j=0}^{k-1} e^{(-i\sigma_{\alpha} + \Gamma_{\alpha})jP_{\text{orb}}} = \frac{e^{(i\sigma_{\alpha} - \Gamma_{\alpha})P_{\text{orb}}/2}}{1 - e^{(i\sigma_{\alpha} - \Gamma_{\alpha})P_{\text{orb}}}} \left[ 1 - e^{(i\sigma_{\alpha} - \Gamma_{\alpha})kP_{\text{orb}}} \right] (\Delta a_{\alpha}), \quad (50)$$

where  $\Delta a_{\alpha}$  is the change of mode amplitude in the first periastron passage when there is no initial oscillation [cf. Eq. (28)]

$$\Delta a_{\alpha} = \frac{GM'W_{lm}Q_{\alpha}}{2i(\sigma_{\alpha} - B_{\alpha})} \int_{-P_{\text{orb}}/2}^{P_{\text{orb}}/2} dt \frac{e^{-im\Phi - i\sigma_{\alpha}t}}{D^{l+1}} = \frac{\pi GM'Q_{\alpha}}{iD_p^{l+1}(\sigma_{\alpha} - B_{\alpha})} K_{lm}(\sigma_{\alpha}). \quad (51)$$

Clearly, when  $kP_{\text{orb}}\Gamma_{\alpha} \gg 1$ , the amplitude  $a_{\alpha}(t_k)$  becomes independent of  $k$ . The steady-state mode energy is given by

$$\langle E_{\alpha} \rangle = \frac{\Delta E_{\alpha}}{2 [\cosh(\Gamma_{\alpha}P_{\text{orb}}) - \cos(\sigma_{\alpha}P_{\text{orb}})]} \simeq \frac{\Delta E_{\alpha}}{4 \sin^2(\sigma_{\alpha}P_{\text{orb}}/2) + (\Gamma_{\alpha}P_{\text{orb}})^2}, \quad (52)$$

where  $\Delta E_\alpha = (GM'^2 R^5 / D_p^6) \pi^2 |Q_\alpha K_{lm}(\sigma_\alpha)|^2 \sigma_\alpha / (\sigma_\alpha - B_\alpha)$  is the energy transferred to the mode in the first periastron. Equation (52) establishes the relationship between steady-state tidal energy  $\langle E_s \rangle = \sum_\alpha \langle E_\alpha \rangle$  and the initial energy transfer  $\Delta E_s = \sum_\alpha \Delta E_\alpha$ . Typically we have  $\langle E_s \rangle \simeq \Delta E_s$ , except when a mode is in close resonance with the orbit, i.e.,  $\sigma_\alpha = 2\pi N / P_{\text{orb}} = N\Omega_{\text{orb}}$  (where  $N$  is an integer).

## 6.2. Orbital Resonances

We now consider the probability that the orbital evolution is driven by a near orbital resonance  $\sigma_\alpha P_{\text{orb}} = 2(N + \varepsilon)\pi$ , with  $|\varepsilon| \ll 1$ . For the modes which contribute significantly to the energy transfer,  $\sigma_\alpha \gtrsim 2\Omega_p$ , thus  $N = \sigma_\alpha / \Omega_{\text{orb}} \gtrsim 2(1 + e)^{1/2} / (1 - e)^{3/2} \simeq 32$ . For  $\langle E_\alpha \rangle \geq 10\Delta E_\alpha$  we require  $|\varepsilon| \leq 0.05$ , and we use this to define the full width  $(\Delta P_{\text{orb}})_\varepsilon$  (in the  $P_{\text{orb}}$ -space) of the resonance:  $(\Delta P_{\text{orb}} / P_{\text{orb}})_\varepsilon = 2\varepsilon / N$ . Suppose the energy transfer is dominated by a single mode  $\alpha$ , then the time the orbit spends near resonance is  $(\Delta t)_\varepsilon = (8\pi^2 \varepsilon^3 / 3N) t_{\text{decay}}$ , where  $t_{\text{decay}} = |P_{\text{orb}} / \dot{P}_{\text{orb}}|$  with  $\dot{P}_{\text{orb}}$  evaluated assuming  $\langle E_s \rangle \simeq \langle E_\alpha \rangle = \Delta E_\alpha$ . On the other hand, the times it takes the orbit to evolve between resonances is  $(\Delta t)_r = (2/N) t_{\text{decay}}$ . Clearly, the ratio  $(\Delta t)_\varepsilon / (\Delta t)_r = (4\pi^2 / 3) \varepsilon^3$  is much less than unity. Therefore it is unlikely that the orbital decay is driven by such a close resonance (see also KQ). In the following, we shall set  $\langle E_\alpha \rangle \simeq \Delta E_\alpha$ .

## 6.3. Retrograde vs. Prograde Rotations

Figure 8 shows the dimensionless quantities [cf. Eqs. (22) and (25)]  $T_2^{(r)} = T_{22}^{(r)}$  (energy transfer in the rotating frame),  $S_2 = S_{22}$  (angular momentum transfer) and  $T_2 = T_{22}$  (energy transfer in the inertial frame) as a function of the stellar rotation rate (for  $\eta = 7$ , corresponding to neutron star mass  $M' = 1.4$  and orbital semimajor axis  $20R$ ). All g-modes with  $n = 1, 2, \dots, 20$  are included in our calculations. As in parabolic tidal encounters (§5), we find that retrograde rotation increases the tidal energy significantly because energy transfer is shifted from higher-order to lower-order g-modes. We can see this effect clearly in Fig. 9, which shows contributions of different modes to the energy transfer for several different rotation rates: At  $\Omega_s = 0$ , the dominant modes are g<sub>6</sub>-g<sub>8</sub>, while for  $\Omega_s = -0.4$ , they are shifted to g<sub>3</sub>-g<sub>5</sub>. As a result,  $\Delta E_s$  for  $\Omega_s = -0.4$  is 24 times larger than the nonrotating value.

We see from Fig. 8 that moderate prograde rotation ( $\Omega_s > 0$ ) decreases  $\Delta J_s$  and  $\Delta E_s$ , and for sufficiently large  $\Omega_s$ , both  $\Delta J_s$  and  $\Delta E_s$  can become negative, i.e., angular momentum and energy are transferred from the star to the orbit, leading to orbital expansion. We find that  $\Delta J_s < 0$  for  $\Omega_s > 0.319$  and  $\Delta E_s < 0$  for  $\Omega_s > 0.362$ . These critical  $\Omega_s$ 's are larger than  $\Omega_p = 0.192$ , the orbital frequency at periastron <sup>5</sup>. Although this result agrees qualitatively with that of KQ, there

---

<sup>5</sup>The measured surface velocity of the B-star in the PSR J0045-7319 binary is 113 km/s (Bell et al. 1995). This

are significant quantitative differences: KQ found that  $\Delta E_s$  changes sign at  $\Omega_s/\Omega_p = 1.2$  (from their Fig. 1 and note that they used stellar radius  $R = 6R_\odot$ ) whereas we find  $\Omega_s/\Omega_p = 1.9$ <sup>6</sup>. Moreover, KQ found that at extreme rotation rate (say  $\Omega_s > 0.4$ ) the magnitude of the energy transfer is larger than the nonrotating value (and they have concluded that prograde rotation can also explain the observed orbital evolution timescale, although with a wrong sign), whereas we find that  $|\Delta E_s|$  is much less than the nonrotating value even at  $\Omega_s = 0.5$ . We think these differences mainly come from KQ’s problematic treatment of mode decomposition (particularly the effect of Coriolis force). This is explained in the following paragraphs.

KQ’s results are based on the solution of an approximate mode amplitude equation in the rotating frame:

$$\ddot{a}_\alpha + \omega_\alpha^2 a_\alpha + 2\Gamma_\alpha \dot{a}_\alpha = \frac{GM'W_{lm}Q_\alpha}{D^{l+1}} e^{-im(\Phi-\Omega_s t)}, \quad (53)$$

(only  $l = 2$  tides are considered). While they included the corrections to  $\omega_\alpha$  and  $Q_\alpha$  from the Coriolis force, KQ neglected the corresponding Coriolis force term, proportional to  $(\dot{a}_\alpha - i\omega_\alpha a_\alpha)$ , in Eq. (53). Decomposing the external forcing  $e^{-im\Phi}/D^{l+1}$  into Fourier components with frequencies equal to multiples of  $\Omega_{\text{orb}}$ , we find that the steady-state mode amplitude is given by

$$a_\alpha = \frac{GM'Q_\alpha}{D_p^{l+1}} \exp(im\Omega_s t) \sum_{k=-\infty}^{\infty} \frac{K_{lm,k} \exp(ik\Omega_{\text{orb}} t)}{\omega_\alpha^2 - (m\Omega_s + k\Omega_{\text{orb}})^2 + 2\Gamma_\alpha(m\Omega_s + k\Omega_{\text{orb}})i} \quad (54)$$

where  $K_{lm,k} \equiv \Omega_{\text{orb}} K_{lm}(k\Omega_{\text{orb}})$ . The mode amplitude in the inertial frame is simply  $a_\alpha e^{-im\Omega_s t}$ . Note that  $K_{lm,k}$  is very small when  $m$  and  $k$  have the same signs, thus for  $m > 0$  we can neglect the positive- $k$  terms in the sum, and for  $m < 0$  neglect the negative- $k$  terms. Equation (54) is then equivalent to Eq. (1) of KQ (see also Kumar, Ao & Quataert 1995). However, it is easy to see that this expression is problematic: According to Eq. (54), even at the apocenter, the mode does not oscillate at its intrinsic frequency ( $\omega_\alpha$  in the rotating frame), and yet its amplitude still depends on the intrinsic mode quantities  $\omega_\alpha$  and  $Q_\alpha$  (which are dependent on the pattern speed of the mode).

To see the problem more clearly, we can calculate the energy transfer and angular momentum transfer in the “first” periastron passage. As shown in §6.1, in the absence of close orbital resonance (§6.2), these are approximately equal to the steady-state mode energy and angular momentum. Applying the same procedure of §3 to Eq. (53), we obtain the dimensionless tidal

---

corresponds to a rotational angular frequency [in units of  $(GM/R^3)^{1/2}$ ] of  $0.22/\sin i_{sn}$  (where  $i_{sn}$  is the angle between the spin axis and the line-of-sight). The component of  $\Omega_s$  perpendicular to the orbital plane is  $(0.22/\sin i_{sn}) \cos \beta$ , where the spin-orbit inclination angle  $\beta$  is constrained to be in the range  $25^\circ < \beta < 55^\circ$  or  $125^\circ < \beta < 155^\circ$  (Kapsi et al. 1996; note that the other constraint,  $\beta < 41^\circ$  or  $\beta > 139^\circ$ , is effective only if we restrict the orbital precession phase angle to the first or the third quadrants).

<sup>6</sup>This is different from static tide where  $\dot{E}_{\text{orb}}$  and  $\dot{J}_{\text{orb}}$  change sign at  $\Omega_s \simeq \Omega_p$ : The weak friction theory (Alexander 1973; Hut 1981) gives  $\dot{E}_{\text{orb}} \propto -[1 - f(e)\Omega_s/\Omega_p]$  and  $\dot{J}_{\text{orb}} \propto -[1 - g(e)\Omega_s/\Omega_p]$ , where  $f = 1, 0.979, 0.957$  and  $g = 1, 1.216, 1.212$  for  $e = 0, 0.808, 1$ .

energy and angular momentum:

$$T_2^{(r)} = \pi^2 \sum_{\alpha} Q_{\alpha}^2 \left[ |K_{2m}(\omega_{\alpha} - m\Omega_s)|^2 + |K_{2-m}(\omega_{\alpha} + m\Omega_s)|^2 \right], \quad (55)$$

$$S_2 = \pi^2 \sum_{\alpha} Q_{\alpha}^2 \left( -\frac{m}{\omega_{\alpha}} \right) \left[ |K_{2m}(\omega_{\alpha} - m\Omega_s)|^2 - |K_{2-m}(\omega_{\alpha} + m\Omega_s)|^2 \right], \quad (56)$$

$$T_2 = \pi^2 \sum_{\alpha} \frac{Q_{\alpha}^2}{\omega_{\alpha}} \left[ (\omega_{\alpha} - m\Omega_s) |K_{2m}(\omega_{\alpha} - m\Omega_s)|^2 + (\omega_{\alpha} + m\Omega_s) |K_{2-m}(\omega_{\alpha} + m\Omega_s)|^2 \right]. \quad (57)$$

It is easy to see that Eqs. (56)-(57) are identical to Eqs. (26) and (23) with  $B_{\alpha} = -m\Omega_s$  (i.e., with the Coriolis term neglected). For comparison, we also plotted in Fig. 8 the numerical results calculated using these expressions, which are in reasonable agreement with KQ's (see their Fig. 1). However, these expressions are certainly *incorrect*, as they would imply that a prograde mode and retrograde mode have the same frequencies in the rotating frame. Indeed, integrating Eq. (53) directly we find that after the first peristron passage, the mode amplitude (in the rotating frame) is a superposition of  $e^{im\phi+i\omega_{\alpha}t}$  and  $e^{im\phi-i\omega_{\alpha}t}$  — This is clearly unphysical. It is easy to show that the erroneous expressions (55)-(57) lead to overestimates of the negative angular momentum and energy transfers for prograde stellar rotation.

#### 6.4. Long-Term Orbital Evolution

In the steady state, the energy transferred to a stellar mode in each periastron passage is equal to the mode energy dissipated in one orbit,  $2\Gamma_{\alpha}P_{\text{orb}}\langle E_{\alpha} \rangle \simeq 2\Gamma_{\alpha}P_{\text{orb}}\Delta E_{\alpha}$ . The corresponding angular momentum transfer is  $2\Gamma_{\alpha}P_{\text{orb}}\Delta J_{\alpha}$ . Thus the orbital energy and angular momentum decay rates are given by

$$\frac{d\langle E_{\text{orb}} \rangle}{dt} = - \sum_{\alpha} 2\Gamma_{\alpha}\langle E_{\alpha} \rangle \simeq - \sum_{\alpha} 2\Gamma_{\alpha}\Delta E_{\alpha}, \quad (58)$$

$$\frac{d\langle J_{\text{orb}} \rangle}{dt} \simeq - \sum_{\alpha} 2\Gamma_{\alpha}\Delta J_{\alpha} = - \frac{d\langle J_s \rangle}{dt}. \quad (59)$$

If we define the mean damping time  $t_{\text{damp}}$  via  $\sum_{\alpha} \Gamma_{\alpha}\Delta E_{\alpha} = \Delta E_s/t_{\text{damp}}$ , then the current orbital decay rate is given by

$$\frac{\dot{P}_{\text{orb}}}{P_{\text{orb}}} \simeq -(0.5 \text{ Myr})^{-1} \left( \frac{T_2}{10^{-2}} \right) \left( \frac{30 \text{ yr}}{t_{\text{damp}}} \right). \quad (60)$$

Note that  $T_2 = 10^{-2}$  corresponds to nearly maximum retrograde rotation. Thus to explain the observed  $\dot{P}_{\text{orb}}$ , the damping times of the dominant modes ( $g_3$ - $g_5$ ; cf. Fig. 9) must be less than 30 years. As pointed out by KQ, such a short radiative damping time is unlikely if the star is rigidly rotating, but would be possible if there is differential rotation. Such differential rotation is naturally expected since tidal torque deposits angular momentum mainly in the region near the stellar surface (Goldreich & Nicholson 1989).

Independent of the mode damping rates, equations (58) and (59) provide a scaling relation for the orbital decay rate as a function of the orbital and spin parameters. For  $4 < \eta < 10$ , we can fit the function  $T_2$  by  $T_2 \propto \eta^{-4\nu}$ , where  $\nu$  depends mainly on  $\Omega_s$  but only slightly on the eccentricity (as long as  $e \gtrsim 0.7$ ): we find  $\nu = 1, 0.5, 0.2$  for  $\Omega_s = 0, -0.2, -0.4$  (see Fig. 4). We then have

$$\frac{\dot{P}_{\text{orb}}}{P_{\text{orb}}} \propto -P_{\text{orb}}^{-10/3-4\nu} (1-e)^{-6(1+\nu)}, \quad (61)$$

where the proportional constant can be fixed by the current observed value of  $\dot{P}_{\text{orb}}$ . Similar equations for  $\dot{e}$  and  $\dot{\Omega}_s$  are easily obtained. These equations can be used to infer the long-term evolution of the binary system. Note that since  $\Delta E_s \simeq \beta(GM/R^3)^{1/2} \Delta J_s$ , where  $\beta$  is of order unity (for the current system,  $\eta = 7$ , we find  $\beta = 3$  for  $\Omega_s = 0$  and  $\beta = 5$  for  $\Omega_s = -0.5$ ), the rates at which  $J_{\text{orb}}$  and  $J_s$  change are given by

$$\left| \frac{\dot{J}_{\text{orb}}}{J_{\text{orb}}} \right| = \frac{\beta}{3} \left( \frac{1-e}{1+e} \right) \Omega_p \left| \frac{\dot{P}_{\text{orb}}}{P_{\text{orb}}} \right|, \quad \left| \frac{\dot{J}_s}{J_s} \right| = \frac{0.50\beta(1-e)}{\lambda(1+e)^{1/3}} \Omega_p^{2/3} \Omega_s^{-1} \left| \frac{\dot{P}_{\text{orb}}}{P_{\text{orb}}} \right|, \quad (62)$$

where we have taken the moment of inertia  $I = 0.1\lambda MR^2$ , and  $\Omega_s$  and  $\Omega_p$  are in units of  $(GM/R^3)^{1/2}$ . Both  $|\dot{J}_{\text{orb}}/J_{\text{orb}}|$  and  $|\dot{J}_s/J_s|$  are much smaller than  $|\dot{P}_{\text{orb}}/P_{\text{orb}}|$ , i.e., the timescale for changing the orbital angular momentum and the timescale for synchronizing and aligning the stellar spin are much longer than the orbital decay time<sup>7</sup>. The orbit therefore evolves with decreasing orbital period and eccentricity, while the periastron distance  $D_p$  remains approximately constant. Since  $\Delta E_s$  mainly depends on  $D_p$ , the orbital decay rate  $|\dot{P}_{\text{orb}}/P_{\text{orb}}| \propto \Delta E_s/|E_{\text{orb}}|$  was larger at earlier times (when  $|E_{\text{orb}}|$  was smaller). This implies that there is an upper limit to the age of the binary since the neutron star formation. Integrating the parametrized evolutionary equations backward in time, we find that regardless of the various uncertainties, the orbital age is always less than 1.4 Myr (Lai 1996). This is significantly smaller than the characteristic age (3 Myr) of the pulsar, implying that the latter is not a good age indicator. The most likely explanation for this discrepancy is that the initial spin period of the pulsar is close to its current value. Thus the pulsar was either formed rotating very slowly, or has suffered spin-down due to accretion in the first  $\sim 10^4$  years (the Kelvin-Holmholz time of the B-star) after the supernova (E. van den Heuvel 1996, private communication).

## 7. Discussion

The main result of this paper has been summarized in the abstract. Here we simply note that our study of dynamical tides in rotating stars is based on an approximate scheme

---

<sup>7</sup>This is different from evolution driven by static tide, for which  $\dot{E}_{\text{orb}} \simeq \Omega_p \dot{J}_{\text{orb}}$ , and we can show that in this case  $|\dot{J}_{\text{orb}}/J_{\text{orb}}|$  and  $|\dot{J}_s/J_s|$  are larger than those given in Eq. (62) by a factor  $\Omega_p^{-1}$  (although both are still less than  $|\dot{P}_{\text{orb}}/P_{\text{orb}}|$ ).

of mode decomposition, which we believe gives physically meaningful results. Nevertheless, a mathematically rigorous theory describing the response of individual modes in rotating stars to external forcing is highly desirable, and the role of the continuous mode spectrum (Dyson & Schutz 1979) need to be clarified.

In addition to the two applications (tidal capture binary formation and the orbital evolution of pulsar binaries) examined in this paper, tidal excitation of oscillation modes may also be important in the final phase of inspiraling neutron star binaries. Extracting gravitational wave signals from noise requires accurate theoretical waveforms in the frequency range 10 – 1000 Hz, corresponding to the last few minutes of the binaries’ life (Cutler et al. 1993). For nonrotating neutron star, the orbital phase error induced by resonant excitation of g-mode is negligible (Reisenegger & Goldreich 1994; Lai 1994). With rapid rotation, the f-mode frequency in the inertial frame can be significantly reduced, therefore resonant excitation of f-mode is possible even at large orbital separation. We wish to study this and related issues in a future paper.

I thank Pawan Kumar for sending me his papers prior to publication and several interesting conversations. I also thank Lars Bildsten, Lee Linblom and Greg Ushomirsky for discussing modes in rotating stars. This research is supported by the Richard C. Tolman Fellowship at Caltech, NASA Grant NAG 5-2756, and NSF Grant AST-9417371.

### A. Equations for General Spin-Orbit Inclination Angle

In the main body of our paper we assume for simplicity that  $\Omega_s$  is aligned with the orbital angular momentum. Generalization to the cases of arbitrary spin-orbit inclination angle is straightforward. Define a coordinate system  $(xyz)$  centered on  $M$  with the  $z$ -axis along the orbital angular momentum and the  $x$ -axis pointing to the pericenter in the orbital plane. Define another coordinate system  $(x'y'z')$  with the  $z'$ -axis along  $\Omega_s$  and the  $y'$ -axis in the orbital plane. Let the angle between the  $z$ -axis and  $z'$ -axis be  $\beta$  (the spin-orbit inclination angle), and the angle between the  $y$ -axis and  $y'$ -axis be  $\alpha$ . Thus the  $(x'y'z')$  frame is related to the  $(xyz)$  frame by Euler angle  $(\alpha, \beta, \gamma = 0)$ . The function  $Y_{lm}(\theta, \phi)$  is related to  $Y_{lm'}(\theta', \phi')$  by

$$Y_{lm}(\theta, \phi) = \sum_{m'} \mathcal{D}_{m'm}^{(l)}(\alpha, \beta) Y_{lm'}(\theta', \phi'), \quad (\text{A1})$$

where the Wigner  $\mathcal{D}$ -function is given by

$$\begin{aligned} \mathcal{D}_{m'm}^{(l)}(\alpha, \beta) &= e^{im'\alpha} [(l+m)!(l-m)!(l+m')!(l-m')!]^{1/2} \\ &\times \sum_k \frac{(-1)^{l+m'-k} \left(\cos \frac{1}{2}\beta\right)^{2k-m-m'} \left(\sin \frac{1}{2}\beta\right)^{2l-2k+m+m'}}{k! (l+m-k)! (l+m'-k)! (k-m-m')!}, \end{aligned} \quad (\text{A2})$$

(e.g., Wybourne 1974). The mode amplitude equation (5) should then be replaced by

$$\ddot{a}_\alpha + \sigma_\alpha^2 a_\alpha - 2iB_\alpha(\dot{a}_\alpha - i\sigma_\alpha a_\alpha) + 2\gamma_\alpha \dot{a}_\alpha = \sum_{lm'} \frac{GM'W_{lm'}Q_{\alpha l}}{D^{l+1}} \mathcal{D}_{mm'}^{(l)} e^{-im'\Phi}. \quad (\text{A3})$$

It is easy to show that in the egneral cases, equations (28)-(32) still apply, provided that  $K_{lm}(\sigma_\alpha)$  is replaced by

$$\tilde{K}_{lm}(\sigma_\alpha) = \sum_{m'} \mathcal{D}_{mm'}^{(l)} K_{lm'}(\sigma_\alpha), \quad (\text{A4})$$

[recall that  $\alpha = \{n jm\}$ ]. Note that in general, the  $m = \pm 1$  modes also contribute to the tidal excitation (unlike the aligned case, where only the  $m = 0, \pm 2$  modes are excited).

## B. The Functions $Q_{\alpha l}$ and $B_\alpha$

With  $\xi_r(\mathbf{r})$  and  $\delta P(\mathbf{r})$  expressed in Eq. (36), the other eigenfunctions are

$$\delta\rho(\mathbf{r}) = \delta\rho(r)He^{im\phi} = \left( \frac{\delta P}{c_s^2} + \frac{\rho N^2}{g} \xi_r \right) He^{im\phi}, \quad (\text{B1})$$

$$\xi_\theta(\mathbf{r}) = \frac{\xi_\perp(r)}{1 - q^2\mu^2} \left( \frac{\partial H}{\partial\theta} + \frac{mq\mu}{\sin\theta} H \right) e^{im\phi}, \quad (\text{B2})$$

$$\xi_\phi(\mathbf{r}) = \frac{i\xi_\perp(r)}{1 - q^2\mu^2} \left( q\mu \frac{\partial H}{\partial\theta} + \frac{m}{\sin\theta} H \right) e^{im\phi}, \quad (\text{B3})$$

where the mode index  $\alpha = \{n jm\}$  has been suppressed,  $q = 2\Omega_s/\omega_\alpha$ ,  $\mu = \cos\theta$ , and  $\xi_\perp(r) = (\delta P)/(\rho r\omega^2)$ . We normalize the Hough function via  $\int d\Omega H^2(\theta) = 2\pi \int d\mu H^2 = 1$ . The eigenfunction is normalized according to

$$\int d^3x \rho \vec{\xi}^* \cdot \vec{\xi} = \int_0^R dr r^2 \rho \left( \xi_r^2 + \Lambda \xi_\perp^2 \right) = 1, \quad (\text{B4})$$

where

$$\Lambda = 2\pi \int_{-1}^1 \frac{d\mu}{(1 - q^2\mu^2)^2} \left[ (1 + q^2\mu^2)(1 - \mu^2) \left( \frac{\partial H}{\partial\mu} \right)^2 + \frac{m^2(1 + q^2\mu^2)}{1 - \mu^2} H^2 - 4mq\mu H \left( \frac{\partial H}{\partial\mu} \right) \right]. \quad (\text{B5})$$

Note that  $\Lambda \rightarrow l(l+1)$  as  $q \rightarrow 0$ . The tidal coupling coefficient defined by Eq. (6) is

$$Q_{\alpha l} = Q_\theta \int_0^R dr r^{l+2} \delta\rho_\alpha(r), \quad Q_\theta = \int d\Omega H e^{-im\phi} Y_{lm}. \quad (\text{B6})$$

The function  $B_\alpha$  defined by Eq. (7) is

$$\begin{aligned} B_\alpha &= -m\Omega_s + 2i\Omega_s \int d^3x \rho \xi_\phi^* (\xi_\theta \cos\theta + \xi_r \sin\theta) \\ &= -m\Omega_s + 2\Omega_s \left( B_{\theta 1} \int_0^R dr r^2 \rho \xi_\perp^2 + B_{\theta 2} \int_0^R dr r^2 \rho \xi_r \xi_\perp \right), \end{aligned} \quad (\text{B7})$$

where

$$B_{\theta 1} = 2\pi \int_{-1}^1 \frac{\mu d\mu}{(1 - q^2\mu^2)^2} \left[ q\mu(1 - \mu^2) \left( \frac{\partial H}{\partial \mu} \right)^2 + \frac{m^2 q \mu}{1 - \mu^2} H^2 - m(1 + q^2\mu^2) H \frac{\partial H}{\partial \mu} \right], \quad (\text{B8})$$

$$B_{\theta 2} = 2\pi \int_{-1}^1 \frac{d\mu}{(1 - q^2\mu^2)} \left[ mH^2 - q\mu(1 - \mu^2) H \frac{\partial H}{\partial \mu} \right]. \quad (\text{B9})$$

Note that  $B_{\theta 1} \rightarrow m/2$  and  $B_{\theta 2} \rightarrow m$  as  $q \rightarrow 0$ .

### C. Asymptotic Expressions for $K_{lm}(\omega)$

For parabolic orbit and in the limit  $y \equiv \eta \sigma \gg 1$  (where  $\sigma = \omega - m\Omega_s$  is the mode frequency in the inertial frame), the functions  $K_{lm}(\sigma)$  can be evaluated analytically. Following PT, we write

$$K_{lm}(\omega) = \frac{\sqrt{2}W_{lm}}{\pi} \eta I_{lm}(y), \quad (\text{C1})$$

$$I_{lm}(y) = \int_0^\infty dx (1 + x^2)^{-l} \cos \left[ 2^{1/2} y(x + x^3/3) + 2m \tan^{-1} x \right]. \quad (\text{C2})$$

Using the method of steepest descents, the integral (C2) can be evaluated in the asymptotic limit ( $y \gg 1$ ). For  $l = 2$ , the leading terms are

$$I_{2-2}(y) = \frac{2\pi^{1/2}}{3} z^{3/2} \exp(-2z/3) \left( 1 - \frac{\pi^{1/2}}{4} z^{-1/2} + \dots \right), \quad (\text{C3})$$

$$I_{20}(y) = \frac{\pi^{1/2}}{4} z^{1/2} \exp(-2z/3) \left( 1 + \frac{\pi^{1/2}}{2} z^{-1/2} + \dots \right), \quad (\text{C4})$$

$$I_{22}(y) = \frac{\pi^{1/2}}{32} z^{-1/2} \exp(-2z/3) \left( 1 - \frac{89}{48} z^{-1} + \dots \right), \quad (\text{C5})$$

where  $z = \sqrt{2}y$  and we have assumed  $y > 0$ . Comparison with numerical integration indicates that these asymptotic expressions are accurate to within 2% for  $y > 2$ .

## REFERENCES

Alexander, M. E. 1973, *Astrophys. and Space Sci.*, 23, 459.

Bell, J. F., Bessell, M. S., Stappers, B. W., Bailes, M. & Kaspi, V. M. 1995, *ApJ*, 447, L117.

Bildsten, L., & Ushomirsky, G., & Cutler, C. 1996, *ApJ*, 460, 827.

Chapman, S., & Lindzen, R. S. 1970, *Atmospheric Tides* (Gordon and Breach: New York).

Cutler, C. et al. 1993, *Phys. Rev. Lett.*, 70, 2984.

Darwin, G. H. 1879, *Phil. Trans. Roy. Soc.*, 170, 1.

Davies, M. B. 1996, in “Dynamics and Evolution of Star Clusters” (IAU Symposium 174), ed. P. Hut and J. Makino.

Dyson, J., & Schutz, B. F. 1979, *Proc. Roy. Soc. London, A.* 368, 389.

Fabian, A. C., Pringle, J. E., & Rees, M. J. 1975, *MNRAS*, 172, 15p.

Goldreich, P., & Nicholson, P. D. 1989, *ApJ*, 342, 1079.

Goldreich, P., & Peale, S. J. 1968, *ARAA*, 6, 287.

Goodman, J., & Oh, S. P. 1997, *ApJ*, submitted (astro-ph/9701006).

Hut, P. 1981, *A&A*, 99, 126.

Hut, P., et al. 1992, *PASP*, 104, 981.

Ipser, J. R., & Lindblom, L. 1990, *ApJ*, 355, 226.

Johnston, S., et al. 1994, *MNRAS*, 268, 430.

Kaspi, V. M., et al. 1994, *ApJ*, 423, L43

Kaspi, V. M., Bailes, M., Manchester, R. N., Stappers, B. W., & Bell, J. F. 1996, *Nature*, 381, 584.

Kaspi, V. M., Tauris, T. M., & Manchester, R. N. 1996, *ApJ*, 459, 717.

Khokhlov, A., Novikov, I. D., & Pethick, C. J. 1993, *ApJ*, 418, 163.

Kochanek, C. S. 1992, *ApJ*, 385, 604.

Kopal, Z. 1978, *Dynamics of Close Binaries* (Reidel, Dordrecht).

Kumar, P., & Goodman, J. 1996, *ApJ*, 466, 946.

Kumar, P., Ao, C. O., & Quataert, E. J. 1995, *ApJ*, 449, 294.

Kumar, P., & Quataert, E. J. 1997, Preprint (KQ).

Lai, D. 1994, *MNRAS*, 270, 611.

Lai, D. 1996, *ApJ*, 466, L35.

Lai, D., Bildsten, L., and Kaspi, V. M. 1995, *ApJ*, 452, 819

Lee, H. M., & Ostriker, J. P. 1986, *ApJ*, 310, 176.

Longuet-Higgins, M. S. 1967, *Phil. Trans. Roy. Soc. London (A)*, 262, 511.

Lyden-bell, D., & Ostriker, J. P. 1967, *MNRAS*, 136, 293.

Managan, R. A. 1986, *ApJ*, 309, 598.

Mardling, R. A. 1995, *ApJ*, 450, 732.

McMillan, S. L., McDermott, P. N., & Taam, R. E. 1987, *ApJ*, 318, 261.

Nicholson, P. N. 1979, Ph.D. Thesis, California Institute of Technology.

Press, W. H., & Teukolsky, S. A. 1977, *ApJ*, 213, 183 (PT).

Provost, J., Berthomieu, G., & Rocca, A. 1981, *A&A*, 94, 126.

Reisenegger, A., & Goldreich, P. 1994, *ApJ*, 426, 688.

Rocca, A. 1989, *A&A*, 213, 114.

Saio, H. 1982, *ApJ*, 256, 717.

Schutz, B. F. 1979, *ApJ*, 232, 874.

Unno, W. et al. 1989, *Nonradial Oscillation of Stars* (Univ. of Tokyo Press).

Wybourne, B. G. 1974, *Classical Groups for Physicists* (John Wiley: New York).

Zahn, J.-P. 1977, *A&A*, 57, 383 (Erratum: 1978, *A&A*, 67, 162).

Table 1: Fitting Parameters for  $T_2$

$\Omega_s$	$A$	$\alpha$
$\Gamma = 4/3$ Model: $T_2 = A \eta^{-\alpha}$		
-0.5	0.25	1.80
-0.4	0.25	2.00
-0.3	0.25	2.26
-0.2	0.25	2.51
-0.1	0.25	2.80
0	0.24	3.1
0.1	0.27	3.6
0.2	0.28	4.1
0.3	0.29	4.6
0.4	0.31	5.2
0.5	0.33	5.8
$\Gamma = 5/3$ Model: $T_2 = A \eta^5 \exp(-\alpha\eta)$		
-0.6	0.51	1.57
-0.4	1.3	1.94
-0.2	3.4	2.34
0	8.1	2.74
0.2	14.	3.10
0.4	24.	3.45
0.6	41.	3.80

**Figure 1** – Frequencies  $\omega$  (in the rotating frame) of selected  $j = 2$  (corresponding to  $l = 2$  in the  $\Omega_s \rightarrow 0$  limit) g-modes as a function of rotation rate  $\Omega_s$ . Both  $\omega$  and  $\Omega_s$  are expressed in units of  $\omega^{(0)}$ , the corresponding mode frequency at zero rotation. The solid curves are for  $m = 0$ , short-dashed curves for  $m = -2$ , and long-dashed curves for  $m = 2$ . For each  $m$ , the four curves correspond g-modes of different radial order:  $g_2$ ,  $g_5$ ,  $g_{10}$  [these curves terminate at  $\Omega_s = 0.5$ ], and  $g_\infty$  (the WKB limit). The numerical results shown in this figure can be fitted by Eqs. (39)-(41).

**Figure 2** – The tidal coupling coefficients  $Q_\alpha = Q_{\alpha 2}$  of selected  $j = 2$  modes as a function of rotation rate  $\Omega_s$  (in units of  $\omega^{(0)}$ , the corresponding mode frequency at zero rotation). The solid curves are for  $m = 0$ , short-dashed curves for  $m = -2$ , and long-dashed curves for  $m = 2$ . For each  $m$ , the three curves correspond g-modes of different radial order:  $g_5$ ,  $g_{10}$  (these curves terminate at  $\Omega_s = 0.5$ ) and  $g_{20}$  (Note that the  $g_5$  curves almost overlap with the  $g_{10}$  curves).

**Figure 3** – The frequencies  $\omega$  and angular coupling coefficients  $Q_\theta$  of selected  $j = 4$  g-modes (heavy curves) compared with those of the  $j = 2$  modes (lighter curves). The solid lines are for  $m = 0$ , short-dashed lines for  $m = -2$  and long-dashed lines for  $m = 2$ . (a) gives the frequency (in the rotating frame)  $\omega$  in the WKB limit ( $n \rightarrow \infty$ ), and (b) shows the quantity  $Q_\theta$  as defined in Appendix B.

**Figure 4** – Dimensionless functions  $T_2^{(r)}$ ,  $S_2$  and  $T_2 = T_2^{(r)} + \Omega_s S_2$  [where  $\Omega_s$  is the rotation rate in units of  $(GM/R^3)^{1/2}$ ] as a function of  $\eta$  for  $\Omega_s = 0$  (solid lines), 0.2 (dotted lines),  $-0.2$  (short-dashed lines), 0.4 (long-dashed lines) and  $-0.4$  (dot-dashed lines) in a parabolic encounter. The star is modeled as a  $\Gamma = 4/3$ ,  $\Gamma_1 = 5/3$  polytrope. Note that for  $\Omega_s = 0.4$  (long-dashed lines),  $S_2$  becomes negative for  $\eta > 5.36$  [see (b)], and  $T_2$  becomes negative for  $\eta > 6.45$  [see (c)].

**Figure 5** – Energy transfer as a function of periastron distance  $D_p$  during an encounter between a main-sequence star  $M = 1M_\odot$ ,  $R = 1R_\odot$  (modelled as a  $\Gamma = 4/3$  polytrope) and a  $M' = 1.4M_\odot$  point mass (neutron star). The four horizontal lines show the kinetic energy at infinity  $\mu v^2/2$  of the two stars with relative velocity  $v = 20$ , 10, 5, 2.5  $\text{km s}^{-1}$ . The solid curve is for  $\Omega_s = 0$ , the dotted curve  $\Omega_s = 0.2$ , the long-dashed curve  $\Omega_s = 0.5$  (close to the maximum rotation rate), the short-dashed curve  $\Omega_s = -0.2$ , and the dot-dashed curve  $\Omega_s = -0.5$ .

**Figure 6** – Energy transfer as a function of periastron distance  $D_p$  during an encounter between a main-sequence star  $M = 1M_\odot$ ,  $R = 1R_\odot$  (modeled as a  $\Gamma = 5/3$  polytrope) and a  $M' = 1.4M_\odot$  point mass (neutron star). The four horizontal lines show the kinetic energy at infinity  $\mu v^2/2$  of the two stars with relative velocity  $v = 20$ , 10, 5, 2.5  $\text{km s}^{-1}$ . The solid curve is for  $\Omega_s = 0$ , the dotted curve  $\Omega_s = 0.3$ , the long-dashed curve  $\Omega_s = 0.6$  (close to the maximum rotation rate), the short-dashed curve  $\Omega_s = -0.3$ , and the dot-dashed curve  $\Omega_s = -0.6$ .

**Figure 7** – Evolution of (a) the energies  $\delta E_{\text{orb}} = E_{\text{orb}} - E_o$  (where  $E_o$  is the initial orbital energy) and  $E_s^{(r)}$  (the mode energy in the rotating frame), and (b) the angular momenta  $\delta J_{\text{orb}} = J_{\text{orb}} - J_o$  (where  $J_o$  is the initial orbital angular momentum) and  $\delta J_s$  (the mode angular momentum) due to dynamical tide with  $\Omega_s = -0.4$ . Only g<sub>2</sub>-g<sub>8</sub> modes are included in the calculation, and relatively large damping rates are chosen for clearer illustration:  $\Gamma_\alpha = 0.1/P_{\text{orb}}$  (heavy lines) and  $\Gamma_\alpha = 0.05/P_{\text{orb}}$  (light lines).

**Figure 8** – Dimensionless tidal energies  $T_2^{(r)}$  (in the rotating frame),  $T_2$  (in the inertial frame) and angular momentum  $S_2$  as a function of the stellar rotation rate  $\Omega_s$  [in units of  $(GM/R^3)^{1/2}$ ]. The dimensionless orbital parameters are  $\eta = 7$  and  $e = 0.808$ . The solid curves are obtained using the correct expressions (31)-(33); the dashed curves are obtained using the same equations but assuming  $B_\alpha = -m\Omega_s$  (i.e., neglecting the Coriolis term) — These demonstrate that our results are insensitive to uncertainties in Eqs. (31)-(33). Note that  $S_2$  and  $T_2$  become negative for  $\Omega_s > 0.311$  and  $\Omega_s > 0.356$  respectively. The dotted curves are obtained using the incorrect expressions (55)-(57); these give results similar to those of KQ.

**Figure 9** – The contributions of g-modes of different order ( $n$ ) to the function  $T_2$  [the dimensionless energy transfer in the inertial frame; cf. Eqs. (22), (31)] for  $\Omega_s = 0$  (triangles),  $\Omega_s = -0.4$  (squares) and  $\Omega_s = 0.4$ . The solid circles indicate positive contributions, the open circles indicate negative ones.

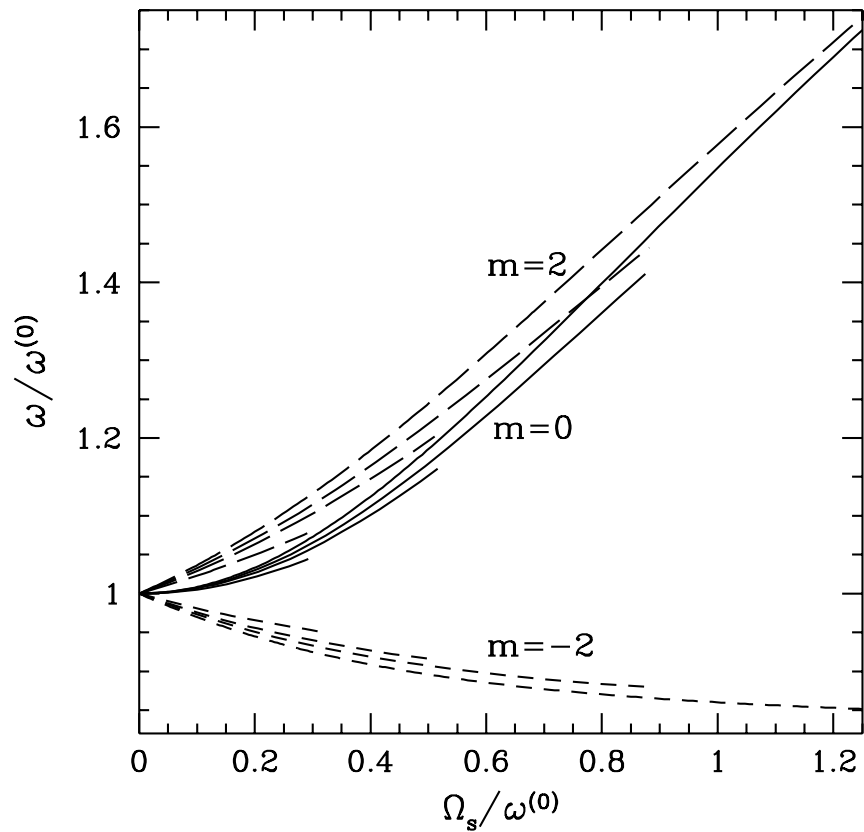


Fig. 1.—

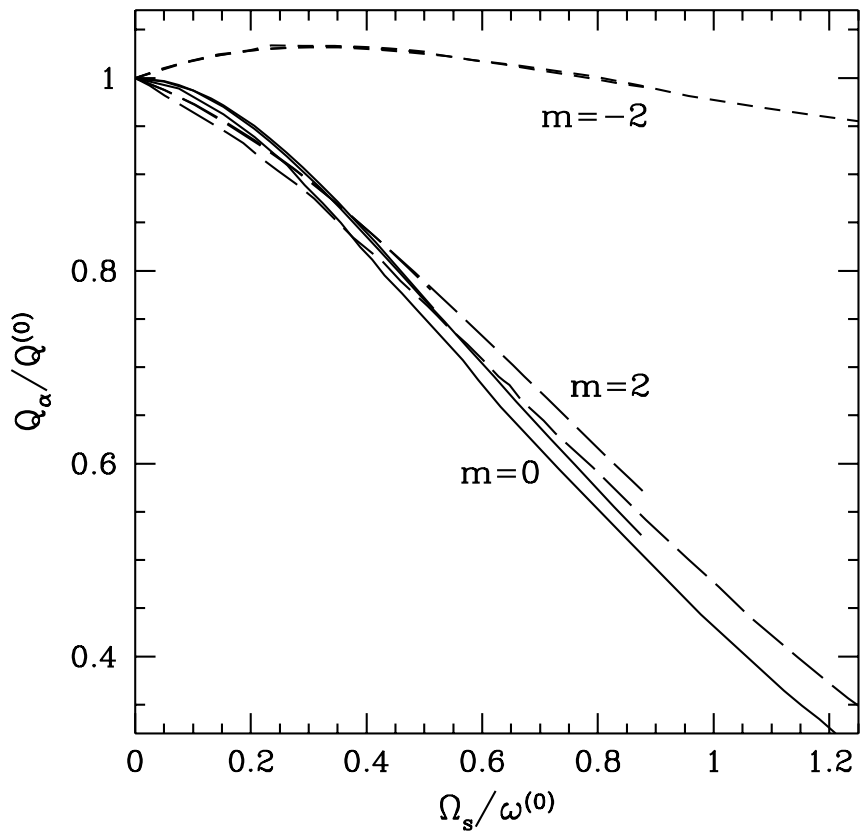


Fig. 2.—

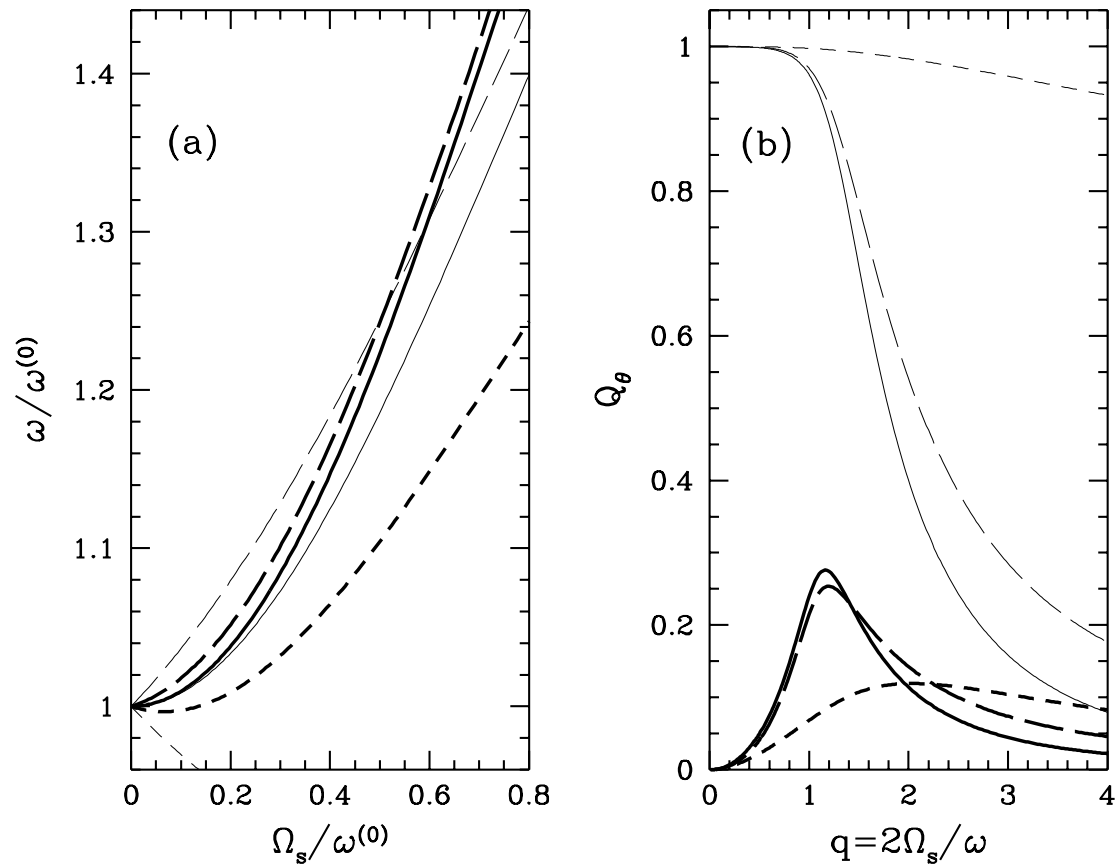


Fig. 3.—

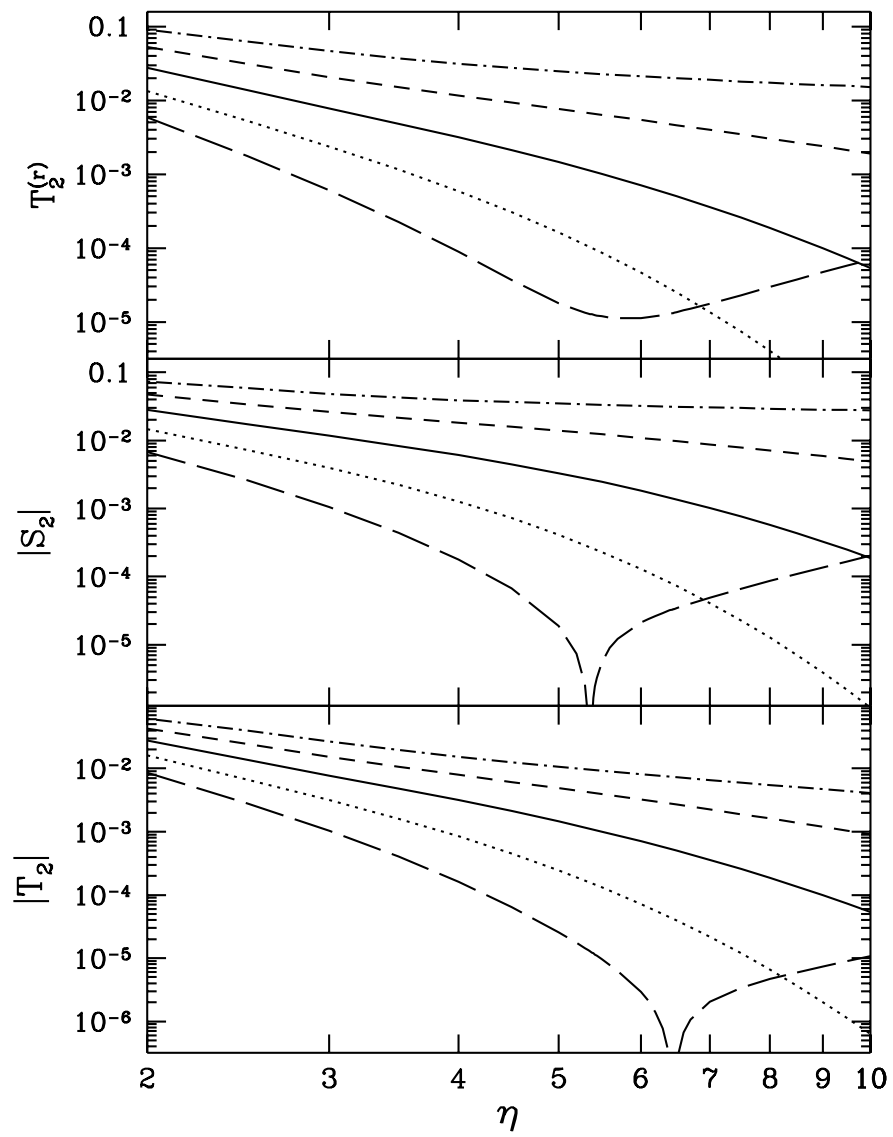


Fig. 4.—

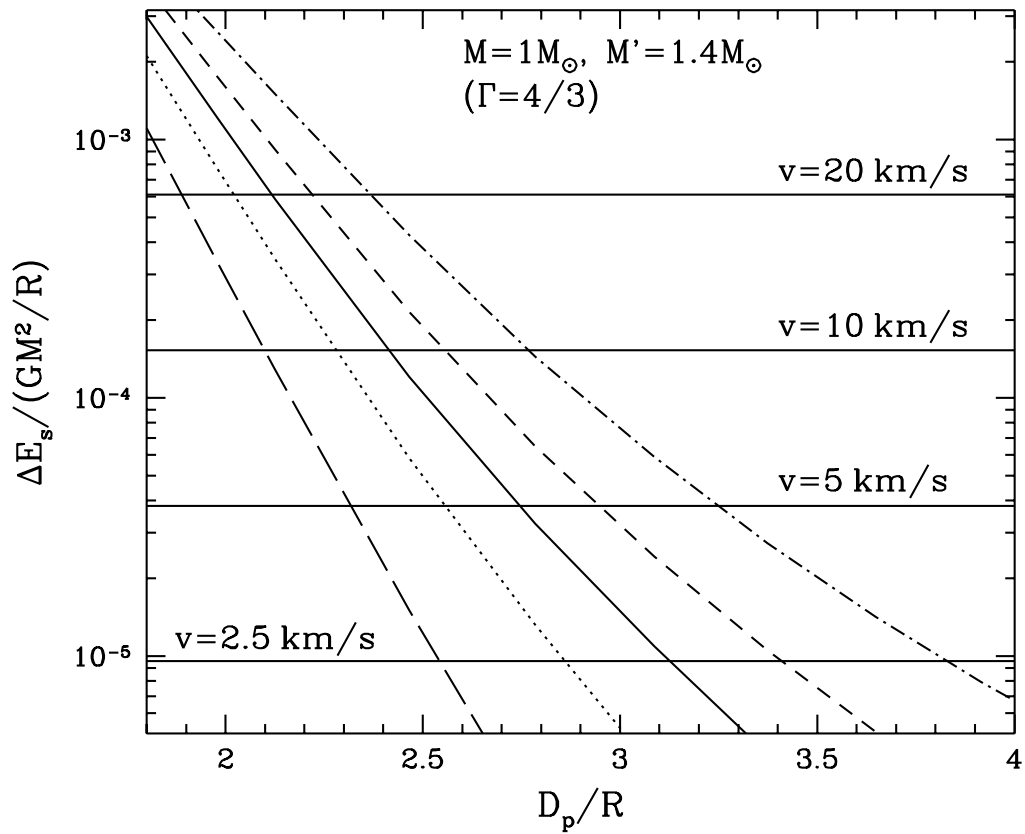


Fig. 5.—

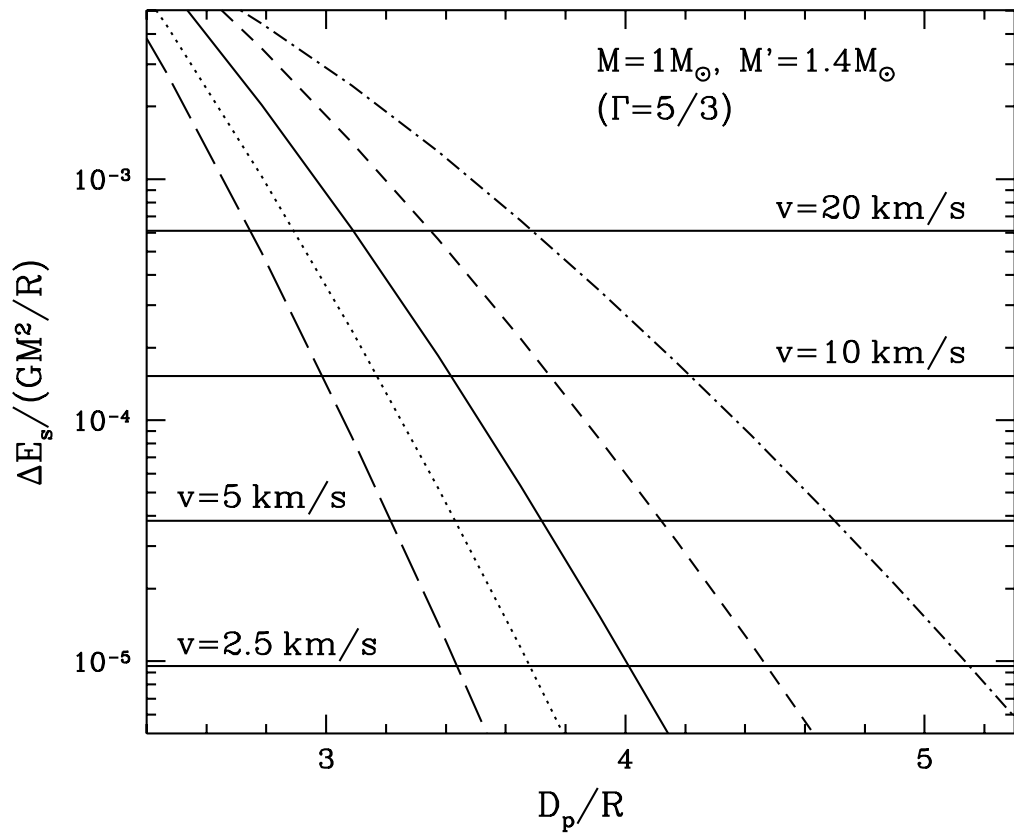


Fig. 6.—

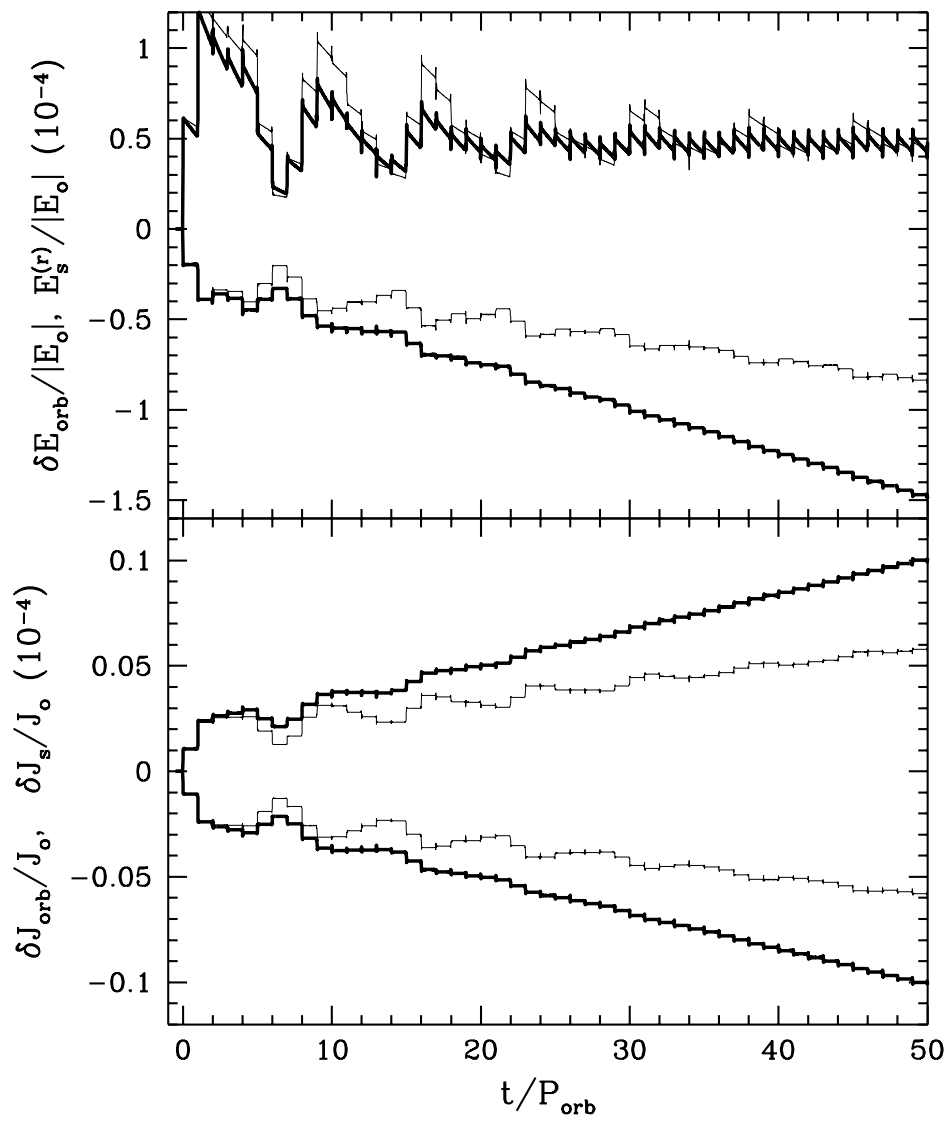


Fig. 7.—

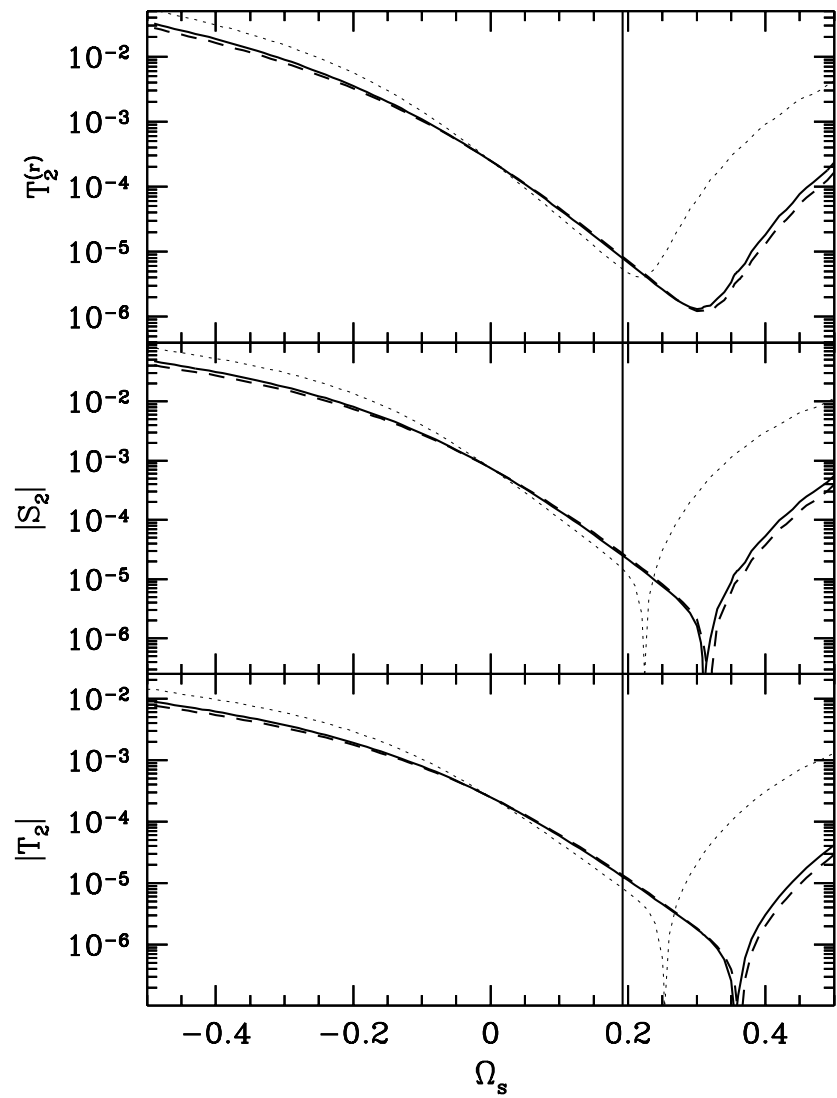


Fig. 8.—

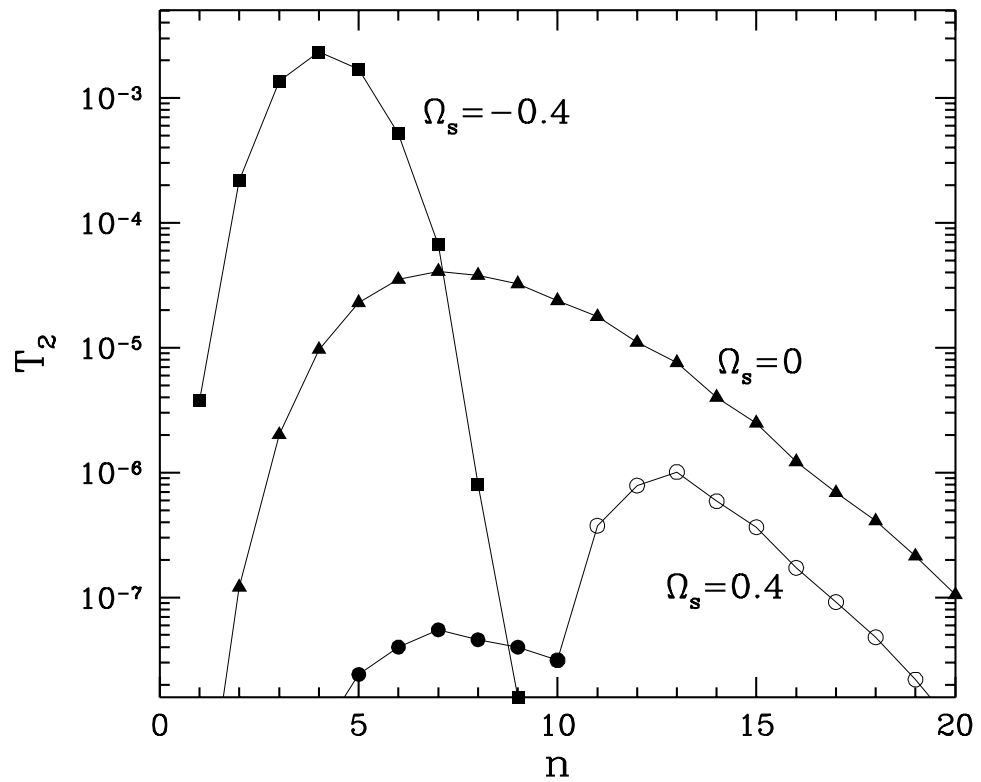


Fig. 9.—